

Neural Network Ground State from the Neural Tangent Kernel Perspective: The Sign Bias

Harel Kol-Namer, Moshe Goldstein

School of Physics and Astronomy, Tel-Aviv University, Tel Aviv 6997801, Israel

Abstract

Neural networks has recently attracted much interest as useful representations of quantum many body ground states, which might help address the infamous sign problem. Most attention was directed at their representability properties, while possible limitations on finding the desired optimal state have not been suitably explored. By leveraging well-established results applicable in the context of infinite width, specifically regarding the renowned neural tangent kernel and conjugate kernel, a comprehensive analysis of the convergence and initialization characteristics of the method is conducted. We reveal the dependence of these characteristics on the interplay among these kernels, the Hamiltonian, and the basis used for its representation. We introduce and motivate novel performance metrics and explore the condition for their optimization. By leveraging these findings, we elucidate a substantial dependence of the effectiveness of this approach on the selected basis, demonstrating that so-called “stoquastic” Hamiltonians are more amenable to solution through neural networks than those suffering from a sign problem.

I. Introduction

Finding the ground state of many-body local spins systems is a notoriously hard task, being QMA complete under pretty mild conditions [1], implying that even with a universal quantum computer one does not expect it to be tractable. Nonetheless, it is believed, and proven for one dimensional gapped systems, that in many physical scenarios with finite range interactions this task should be achievable [2]. While there are many common numerical methods to find the ground state and ground state energy, such as Tensor Networks (TN) or Quantum Monte Carlo (QMC), each has its own strength and weakness and thus applies to only certain classes of Hamiltonians; for example, TN are mostly be used for low dimensional models with a ground state satisfying an area law [3], and QMC suffers from the infamous sign problem, which arises when the Hamiltonian is not stoquastic, as discussed further below.

In recent years the representation of quantum states using neural networks, i.e., Neural Quantum States (NQS), have been proposed and demonstrated success in various tasks [4, 5, 6]. An unnormalized state $|\psi\rangle$ of N spins is represented by a neural network if it can written as

$$|\psi\rangle = \sum_{\sigma} \psi(\sigma, \theta) |\sigma\rangle \quad (1)$$

in some fixed tensor product basis $|\sigma\rangle$ with $\psi(\sigma, \theta) \equiv \psi_{\sigma}$ being the neural network output which we assume to be real without loss of generality¹, given an input $\sigma \in \{-1, 1\}^N$ and the network parameters $\theta \in \mathbb{R}^p$. The output is then fed into a loss function, $\mathcal{L}(|\psi\rangle) : \mathbb{R}^{2^N} \rightarrow \mathbb{R}$, which is minimized via gradient descent (or a variant thereof), through a change of the parameters θ . The task at hand will specify a loss function. In the following we will be interested in the representation of the ground states of local spins Hamiltonian H , hence the chosen loss function will be the energy expectation value $\langle E \rangle \equiv \frac{\langle \psi | H | \psi \rangle}{\langle \psi | \psi \rangle}$.

Allegedly avoiding the limitations of TN and QMC, neural quantum states optimization have been proposed as a promising numerical method for finding the ground state of many-body spins systems. Numerical studies have shown results comparable to other state of the art methods while using various neural networks architectures [4, 9, 10, 11]. Nonetheless it was empirically observed that even though NQS showed success for models such as the

¹As mentioned in [7], every complex k -local Hamiltonian problem can be casted as a $k+1$ -local real Hamiltonian problem. Also in [8] it was shown that if the NTK is complex the dynamics can be separated into two equations, for the real and imaginary parts of the wave functions, with the effective NTKs being the real and imaginary parts of the complex one, each with similar characteristics. For each of those equations our analysis applies.

transverse-field Ising model and other stoquastic Hamiltonians, for non-stoquastic Hamiltonians the performance of this method seems to diminish drastically. While several reasons have been proposed, such as inability to represent states with complex sign structure, Monte Carlo sampling issues, and rugged loss landscape [12, 13, 14, 15], a more comprehensive explanation is sorely missing. It was also noted that whenever possible, a change of basis to one where the Hamiltonian is stoquastic can enhance the performance, indicating that there is an ambiguous dependence on the chosen basis [14][15][16]. Thus, the relationship between the performance of the method and the specific characteristics of the Hamiltonian or the chosen basis remained elusive.

In order to explore those questions we use the highly celebrated infinite width limit [17, 18, 19, 20]. In this limit, neural networks dynamics are often more tractable and enjoy useful features that will be demonstrated later on. We refer to this limit as the Neural Tangent Kernel (NTK) limit. Similar approach have shown to be insightful in the previous works, such as the analysis of quantum neural networks [21, 22] and classical neural networks [8] for quantum state tomography tasks. Similar to our work, geometrical methods have been utilized for analyzing the training dynamics for ground state optimization of NQS such as in [23], yet using different measures such as the Fisher information metric.

The advantage of using the NTK limit in our case is two-fold. We are able to explore the training dynamics in a general setting and the influence of the chosen basis, while eliminating other influences that have been explored, such as the representability capabilities of the network. We are therefore able to demonstrate that NQS suffer from an implicit bias in their initialization and dynamics toward states with a simple sign structure, which we call “the sign bias”. Based on this bias and the special structure of stoquastic Hamiltonians ground states, we are able to explain the hardness in finding the ground states of non-stoquastic Hamiltonians using common NQS training schemes, as compared to TNs.

The study is structured as follows: In Sec. II we outline the general framework and definitions. In Sec. III we review the NTK limit properties based on previous results, and rephrase them in the language of quantum mechanical operators. In Sec. IV we present our general results regarding the interplay between the kernels and the Hamiltonian and its influence on the dynamics and initialization, and build intuition about the desired relations between them. We provide criteria for exponential convergence of the NQS towards the ground state, as well as derive an upper bound on the learning rate in the discrete time case, which might be useful in practice. Based on all these we propose metrics that might predict the success or failure of the method. In Sec. V we discuss what we term the sign “bias”, which might explain why stoquastic Hamiltonians are more amenable to solution using neural networks, and why one can enhance the convergence rate by a change of basis. We also propose metrics that might predict the success or failure of the method and discuss their optimization. In Sec. VI we provide numerical results and demonstrate how the metrics provided are correlated with the convergence speed and initial average values. In Sec. VII we briefly address a commonly used optimization strategy, Stochastic Reconfiguration (SR) as a possible remedy to the sign bias, and more generally, show how one can analyze its strength and limitations using the tools developed throughout the work. Finally, in In Sec. VIII we discuss how our analysis might translate to more general ansatz and exemplify them on TNs, for which we can show that the sign bias does not exist. Some technical details are provided in the Appendixes.

II. General framework and definitions

II.A Neural Networks

Neural network have become very popular in recent years due to their numerous applications [24, 25]. In general, a neural network is a specific case of a parametric function $f(x, \theta_i)$, with x being the input to the network, which might be images of hand written letters, time series, or almost any other object which can be represented digitally. θ_i with $i \in \{1, \dots, p\}$ are the p variational parameters of the network; with different parameters the network represents different functions.

Based on the task at hand, one usually defines a loss function $\mathcal{L} \equiv \mathcal{L}(f(x, \theta))$, which is a functional of the parametric function, and minimizes it by varying the parameters using various gradient descent methods. The most basic gradient descent has the following update rule

$$\theta_i^{n+1} = \theta_i^n - \Delta t \frac{\partial \mathcal{L}}{\partial \theta_i}, \quad (2)$$

with the gradient evaluated at step n and Δt being referred to as the learning rate. The main characteristic of neural networks that distinguish them from other parametric functions is their special recursive form

$$f(x, \theta_i) = h_L(h_{L-1}(h_{L-2}(\dots), \theta_{L-1}), \theta_L), \quad (3)$$

with L being an integer, usually referred to as the number of layers, and h_l being the output of the l th layer, $l = 1 \dots L$, which depends on the subset of parameters θ_l and the previous output h_{l-1} . This structure is what allows for neural networks to be very deep, and thus to represent complicated functions, while still having tractable gradients [26].

In this work we will consider a feedforward neural network with a general number of layers L and an activation function ϕ , as can be seen in Fig. 1, where

$$h_l = \phi(W_l h_{l-1} + b_l), \quad (4)$$

i.e., each layer is composed of an activation function acting element-wise on the results of an affine transformation specified by $W_l \in \mathbb{R}^{p_l \times p_{l-1}}$ and $b_l \in \mathbb{R}^{p_l}$, with p_l being referred to as the width of the l th layer. Each affine transformation acts on the previous hidden units $h_{l-1} \in \mathbb{R}^{p_{l-1}}$, with $h_0 \equiv x \in \mathbb{R}^n$ being the input of the network. We group all of the trainable parameters of the networks and denote it using a vector $\theta \in \mathbb{R}^p$.

We will also mostly consider the continuous time limit of the gradient descent updates in Eq. (2), where it turns into a gradient flow

$$\frac{d\theta_i}{dt} = -\frac{\partial \mathcal{L}}{\partial \theta_i}. \quad (5)$$

Using the chain rule we get an ODE for the state vector

$$\frac{d\psi_\sigma}{dt} = -\sum_{\sigma'} \Theta_{\sigma\sigma'}^t \frac{\partial \mathcal{L}}{\partial \psi_\sigma}, \quad (6)$$

with $\Theta_{\sigma\sigma'}^t = \sum_i \frac{\partial \psi_\sigma}{\partial \theta_i} \frac{\partial \psi_{\sigma'}}{\partial \theta_i}$. The time dependence of $\Theta_{\sigma\sigma'}^t$ makes the analysis of this equation intractable, since the dynamics still depends on the parameters values. Fortunately, recent works in neural networks analysis [17, 18, 19, 20] have shown that when one takes the infinite width limit, i.e., the number of hidden variables in each layer grows to infinity, several useful properties emerge. Their applicability for the energy loss function which we consider here is shown in App. A.

The first property is that Θ , which will be referred to as the NTK in this context, is time independent and completely determined by the initialization and architecture of the network. A second property is that a random initialization of the parameters translates into a normal distribution of the elements of the initial state vector, i.e.,

$$\langle \sigma | \psi^0 \rangle \sim \mathcal{N}(\mu, K), \quad (7)$$

with $|\psi^0\rangle$ being the initial state, and where K is referred to as the Conjugate Kernel (CK), which is determined by the initialization and network architecture. We will consider the case where $\mu = 0$, which corresponds to zero bias initialization.

In our case of interest, and assuming a unique ground state of H (extension to degenerate ground states are possible), the loss function will be the energy loss function

$$\mathcal{L} = \langle E \rangle \equiv \frac{\langle \psi | H | \psi \rangle}{\langle \psi | \psi \rangle}. \quad (8)$$

Hence, using Eq. (6) we get the ODE for the state

$$\frac{d|\psi\rangle}{dt} = \frac{1}{\langle \psi | \psi \rangle} \Theta (\langle E \rangle - H) |\psi\rangle, \quad (9)$$

which will be our main interest throughout the paper. We note that the non-triviality of the kernels is responsible for the basis dependence of the dynamics and initialization. In the case of a trivial NTK, the equation reduces to the imaginary time Schrödinger equation, and would be invariant under basis transformations.

Throughout the paper we disregard the issues which may arise from the use of Monte-Carlo sampling, and since we address the infinite width limit, we can disregard any influence of the representability of the network [26, 17]. These settings thus allow us to eliminate other factors which might influence the capability of neural network in solving the many-body problem and focus on the trainability and dynamics. This in turn will allow us to elucidate the fundamental interplay between the form of the Hamiltonian in a given basis and the architecture of the NQS.

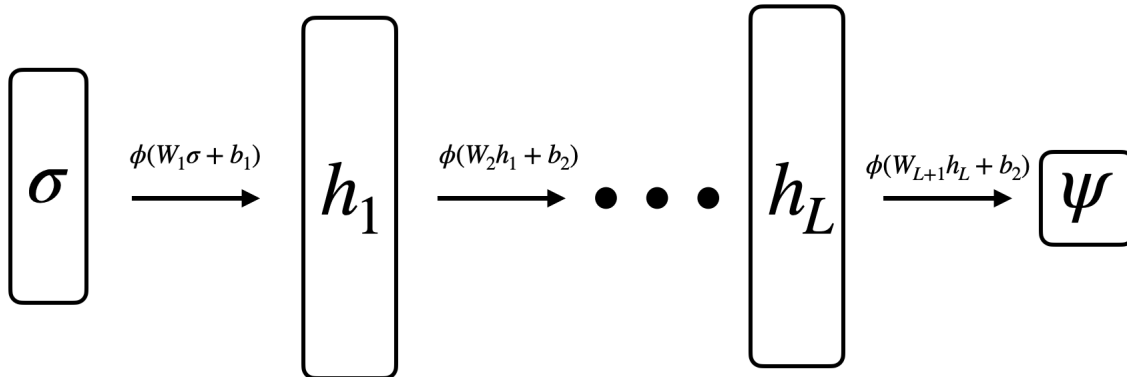


Figure 1: A general fully connected architecture for NQS. The inputs are $\sigma \in \{-1, 1\}^N$, each hidden layer h_l with $l = 1, \dots, L$ represents the output of the affine transformation and non-linear activation, $\phi(W_l h_{l-1} + b_l)$, over the previous layer. The final output is the quantum amplitude of the corresponding spin configuration $\psi(\sigma)$.

II.B Many-Body Spin Hamiltonians

Many-body spin Hamiltonians are the subject of extensive study in fields such as condensed matter physics, high-energy physics, and quantum computation [27, 28]. In our case one can always write them as

$$H = \sum_i^r h_i, \quad (10)$$

with each h_i being a tensor product of Pauli matrices, which we denote by X, Y, Z , and identity matrices. Usually one is concerned with Hamiltonians which have a certain local structure, so we will mostly consider what is known as k -local Hamiltonian. For those Hamiltonians each h_i acts non-trivially on at most k spins or qubits. For example, the Transverse Field Ising Model (TFIM)

$$H_{\text{TFIM}} = -\sum_i h X_i - \sum_{\langle i, j \rangle} Z_i Z_j, \quad (11)$$

is a 2-local Hamiltonian model, with $\langle i, j \rangle$ indicates pairs of nearest neighbors over a general interaction graph.

A known class of Hamiltonians that was first brought up in the context of QMC methods, are stoquastic Hamiltonians:

Definition. *Stoquastic Hamiltonian* - A Hamiltonian is said to be stoquastic in a given tensor-product basis $|\sigma\rangle$ if it satisfies $\langle \sigma | H | \sigma' \rangle \leq 0, \forall \sigma \neq \sigma'$.

An example is the TFIM. Stoquastic Hamiltonians have been an object of interest due to their many special properties and applications. Stoquastic Hamiltonian always have non-negative ground state amplitudes $\langle \sigma | g \rangle \geq 0$, and a Gibbs operator with non-negative matrix elements, $\langle \sigma | e^{-\beta H} | \sigma' \rangle \geq 0, \forall \beta$ in the given basis [29]. Those properties are crucial for the applicability of various QMC methods; and in most cases when the Hamiltonian is non-stoquastic, QMC methods will encounter the notorious sign problem [30]. Since the definition of stoquastic Hamiltonian depends on the basis, in some cases one can attempt to find a different tensor-product basis where the Hamiltonian is stoquastic, although in general this task is NP-hard [31][32].

III. Kernel Properties

We first review previously known properties about the NTK and CK in a more quantum mechanical language, following [17, 33]:

1. Both are positive definite matrices, i.e. $\langle \psi | \Theta | \psi \rangle > 0, \langle \psi | K | \psi \rangle > 0, \forall |\psi\rangle$

2. Their matrix elements are of the form $\langle \sigma | \Theta | \sigma' \rangle = \Phi(\sigma \cdot \sigma')$, $\langle \sigma | K | \sigma' \rangle = F(\sigma \cdot \sigma')$, with $\sigma \in \{-1, 1\}^N$ and Φ , F being functions which depends on the number of layers and activation function that fully characterize the kernels.
3. We define by $X_{|S|} \equiv \sum_{|S|=|S|} X_S$ the sum of all products $X_S = \prod_{i \in S} X_i$ with $S \subset \{1, \dots, N\}$, acting on precisely $|S|$ spins. By the previous property, one can write the kernels in the form $\Theta = \sum_{|S| \leq N} \alpha_{|S|} X_{|S|}$, with $\alpha_{|S|} = \Phi(N - 2|S|)$, and similarly for the CK.
4. It immediately follows from the previous property that the eigenstates of the kernels are the vectors $|s\rangle$ with $s \in \{-, +\}^N$, which are the product states of the X Pauli matrix eigenstates. The eigenvalue associated with each $|s\rangle$ depends only on $|s|$, which we define to be the number of $s_i = -$ in s . Thus, the spectrum of both kernels breaks down to $N + 1$ degenerate subspaces, each with dimension $\binom{N}{|s|}$. We denote the eigenvalue associated with a sector $|s|$ by $\Theta_{|s|}$ and $K_{|s|}$ for the NTK and CK, respectively.
5. “Weak Bias” – The eigenvalues are always ordered as follows

$$\Theta_0 \geq \Theta_2 \geq \dots \geq \Theta_{2k} \geq \dots, \quad (12)$$

$$\Theta_1 \geq \Theta_3 \geq \dots \geq \Theta_{2k+1} \geq \dots,$$

and similarly for the CK. It immediately follows that the maximal eigenvalue of the kernels is either Θ_0 with associated eigenstate $|+\rangle \equiv |+\rangle^{\otimes N}$, or Θ_1 with associated eigenspace spanned by $| -_i \rangle$ with $-_i$ denoting a string of all $+$ except one $-$ sign in the i th position.

6. If $\Phi \geq 0$ then Θ_0 is the maximal eigenvalue, and similarly for the CK.
7. For the CK, if the activation function $\phi > 0$ then $F > 0$. We note that this does not apply in general for the NTK.
8. Denoting by κ_k the k th unique largest eigenvalue of Θ , with a normalization such that $\kappa_1 = 1$, the eigenvalues decay as $\sim \frac{1}{2^{Nk}}$. In the common case where the eigenvalues are ordered by $|s|$ then $\Theta_{|s|} \sim \frac{1}{2^{N|s|}}$.

We mention that as in [33], one can associate a measure of “complexity” for each eigen-space, since each one of them is fully characterized by the number $|s|$, i.e., the number of minus signs in the states $|s\rangle$ which span it. Since for a single qubit $|+\rangle = \frac{1}{\sqrt{2}}(|0\rangle + |1\rangle)$ and $|-\rangle = \frac{1}{\sqrt{2}}(|0\rangle - |1\rangle)$, the number $|s|$ measure the number of dimensions in which the state $|s\rangle$ is “oscillating” while being constant in the other $N - |s|$ dimensions. This notion of complexity stems from the relation to the discrete Fourier Transform, in which a discrete time signal x_n with $n \in \{0, \dots, N - 1\}$ can be decomposed as $x_n = \sum_{k=0}^{N-1} X_k e^{i \frac{2\pi}{N} kn}$. If the significant contributions to the sum comes from large k then the signal is highly oscillating.

IV. Main Results

We begin by discussing the role of the NTK and CK, presenting basic results and their implications, with derivations given in App. B

IV.A The NTK

In order to understand the role of the NTK we discretize the gradient flow defined by Eq. (9),

$$|\psi_{n+1}\rangle = \operatorname{argmin}_{|\psi\rangle} \left\{ \frac{\langle \psi | H | \psi \rangle}{\langle \psi | \psi \rangle} + \frac{1}{2\Delta t} (\langle \psi | - \langle \psi_n |) \Theta^{-1} (|\psi\rangle - |\psi_n\rangle) \right\}, \quad (13)$$

with the index n describing the discrete time step t_n and $\Delta t \equiv t_{n+1} - t_n$. One can see that this is the usual gradient flow, yet instead of having the usual Euclidian metric, the metric is Θ^{-1} , which is the metric induced on the space of the unnormalized state vectors when having the Euclidian metric in parameter space. The dynamics can now be interpreted as follows: at any point $|\psi_n\rangle$ the algorithm searches for the minima of the energy in a small neighborhood defined by the metric Θ^{-1} , which favors changes along directions with small $\langle \Theta^{-1} \rangle$. That bias toward directions with small inverse NTK expectation was noted in previous works in other contexts, such as regression tasks [17, 33, 34]. The severity of that bias depends on the eigenvalues of the kernel. Using Property 5 from the previous section, if Θ_0 or Θ_1 is much larger than any other eigenvalue, the kernel gradient flow will be highly biased.

A similar conclusion can be reached by examining the velocity along the NTK eigenstates. Using Eq. (9) we have

$$\frac{d\langle s|\psi\rangle}{dt} = \Theta_{|s|} \langle s|(\langle E\rangle - H)|\psi\rangle, \quad (14)$$

which can be interpreted as having a generalized gradient flow with a different learning rate in each direction $|s\rangle$, which is proportional to $\Theta_{|s|}$. Thus the flow will be faster along directions with larger $\Theta_{|s|}$.

From the above we formulate the following compatibility conjecture

Conjecture. *Compatibility: For a Hamiltonian H with a ground state $|g\rangle$, the metric $\langle g|\Theta|g\rangle$ is positively correlated with the ease of finding the ground state of H using ANN with NTK Θ .*

In order to lend further support to these ideas, let us consider the specific case that $[H, \Theta] = 0$. Then, denoting the eigenbasis amplitudes of the normalized state by $\frac{\langle E_i|\psi\rangle}{\sqrt{\langle\psi|\psi\rangle}} \equiv \tilde{\psi}_i$ one can show the following

Proposition 1. *If $[H, \Theta] = 0$, a necessary condition for*

$$\frac{d}{dt} \left(\frac{\tilde{\psi}_g^2}{\tilde{\psi}_i^2} \right) > 0$$

is

$$\frac{\langle g|\Theta|g\rangle}{\langle E_i|\Theta|E_i\rangle} > \frac{\langle E\rangle - E_i}{\langle E\rangle - E_g}.$$

For $E_i < \langle E\rangle$ the condition is non-trivial.

Using the above we get that in order for the ground state component to increase relative to the other components, the bias induced toward the ground state relative to other directions cannot be too small. One way to satisfy the criteria $\forall t$ and every eigenstate is to have

$$\langle g|\Theta|g\rangle \gg \langle E_i|\Theta|E_i\rangle, \quad \forall i > 0. \quad (15)$$

For some energy eigenstates or parts of the optimization this criterion is actually necessary. Consider the case where $\langle E\rangle \gg E_i$, which might occur for $|E_i\rangle$ being a low energy eigenstate such as the first excited state and $t \rightarrow 0$, or when we have a relatively small energy gap between the ground state and the first excited state. In that case the necessary condition translates into

$$\frac{\langle g|\Theta|g\rangle}{\langle E_i|\Theta|E_i\rangle} \gtrsim 1, \quad (16)$$

which means that the bias induced toward the ground state must be larger than the bias toward other low energy eigenstates. Otherwise, the energy might decrease, yet due to the NQS becoming more similar to a low energy excited state rather than to the ground state. Only when $\langle E\rangle \approx E_i$ after significant time elapsed, will the NQS start to become more similar to the ground state. Thus, it is preferable that the NTK expectation over the ground state will be much larger than the expectation over the other energy eigenstates, and in some cases this is even necessary in order to achieve reasonable convergence times.

Given some value of $\langle g|\Theta|g\rangle$, one should ask how the NTK expectation values for the other energy eigenstates influence the dynamics. This can be understood from the solution for Eq. (9) near the ground state, i.e. $|\psi\rangle = |g\rangle + \epsilon|\phi\rangle$ with $\epsilon \ll 1$ and the initial perturbation $|\phi_0\rangle$ satisfying $\langle g|\phi_0\rangle = 0$ and $\langle\phi_0|\phi_0\rangle = 1$,

$$|\psi\rangle = |g\rangle + \epsilon\sqrt{\Theta}e^{-\sqrt{\Theta}[H-E_g]\sqrt{\Theta}t}\sqrt{\Theta^{-1}}|\phi_0\rangle, \quad (17)$$

where we assumed without loss of generality that the norm at $t \rightarrow \infty$ is 1, see App. B for further details. From the solution one can see that the convergence to the ground state will be dictated by the eigenvalues of $\tilde{H} = \sqrt{\Theta}[H-E_g]\sqrt{\Theta}$. This matrix is positive definite, so its ground state is $\sqrt{\Theta^{-1}}|g\rangle$ with eigenvalue 0. Denoting the eigenvalues of \tilde{H} by α_i

$$\epsilon^2\alpha_1\langle\phi_0|\sqrt{\Theta^{-1}}|\alpha\rangle^2 e^{-2\alpha_1 t} \leq |\langle E\rangle - E_g| \leq \epsilon^2\langle\phi_0|[H-E_g]|\phi_0\rangle\alpha e^{-2\alpha_1 t} \quad (18)$$

with $|\alpha_1\rangle$ being the first excited state of \tilde{H} with eigenvalue α_1 . Thus, the energy converges to the ground state as $\sim e^{-2\alpha_1 t}$, and so the larger α_1 the fastest the convergence will be.

We are interested in maximizing α_1 given an Hamiltonian. As we show in App. B, it can be seen that this maximum occurs when $\alpha_i = C$ is independent of i for $i > 0$. We also show that it means that $\langle \Theta \rangle_{|E_i\rangle} \propto \frac{1}{E_i - E_g}$ for $i > 0$. This result provides an indication that a desirable relation between the Hamiltonian and the NTK is such that their spectra are inversely correlated, such that increasing the NTK expectation means decreasing the energy.

The same insight also arises by considering Eq. (9) for the specific case $[H, \Theta] = 0$ and noticing that $\frac{d\psi_i^2}{dt} \propto \langle E_i | \Theta | E_i \rangle (\langle E \rangle - E_i) \psi_i^2$. Thus, ψ_i decays for $E_i > \langle E \rangle$ and increases for $E_i < \langle E \rangle$. Considering low $\langle E \rangle$ close to E_g , high energy components with $E_i \gg \langle E \rangle$ will decay fast due to the proportionality with $\langle E \rangle - E_i$. On the other hand, for low energy components with $E_i \gtrsim \langle E \rangle$, one will need $\langle E_i | \Theta | E_i \rangle$ to be large in order to compensate for the small $\langle E \rangle - E_i$. Since having a large $\langle E_i | \Theta | E_i \rangle$ for low energy eigenstates will also increase the low energy components of the state for large $\langle E \rangle \gg E_g$, we suspect that large bias toward low energy states in general will cause fast energy decay for the entirety of the optimization.

Combining this idea with the previous Compatibility Conjecture we formulate a Strong Compatibility Conjecture

Conjecture. *Strong Compatibility: For a Hamiltonian H with eigenstates $|E_i\rangle$, the convergence rate toward the minimal energy is positively correlated with whether or not the following condition is met*

$$\langle \Theta \rangle_{|g\rangle} \gg \langle \Theta \rangle_{|E_1\rangle} > \dots > \langle \Theta \rangle_{|E_k\rangle} > \dots,$$

i.e., if the task of decreasing the energy is compatible with the task of increasing the NTK expectation.

IV.B The CK

The role of the CK is at the initialization, since it is the covariance matrix of the Gaussian distribution of the initial state. One can see that for a general N qubits normalized state $|x\rangle$

$$\mathbb{E} \left(\frac{\langle \psi | x \rangle^2}{\langle \psi | \psi \rangle_{t=0}} \right) \approx \frac{\langle x | K | x \rangle}{\text{Tr}(K)}, \quad (19)$$

meaning that the initial overlap with the ground state is $\frac{\langle g | K | g \rangle}{\text{Tr}(K)}$ on average, and the approximation should be valid for a large number of qubits, see App. B for the argument. Thus, in general one would like a high expectation value of the CK over the ground state in order for the initial state to be close to the ground state. If either of the eigenvalues K_0 or K_1 is much larger than any other value, then the initialization will be highly biased; for example if $K_0 \gg K_i \forall i > 0$, then $\mathbb{E} \left(\frac{\langle \psi | g \rangle^2}{\langle \psi | \psi \rangle} \right) \approx \langle g | + \rangle^2$.

The average initial energy can also be seen to be

$$\mathbb{E}(\langle E \rangle_{t=0}) \approx \frac{\text{Tr}(KH)}{\text{Tr}(K)}. \quad (20)$$

Thus, again, in order to initialize with a low energy, lower energy states should have high CK expectation values, similarly to the desired relation between the NTK and the Hamiltonian. We note that one can calculate the average initial values of higher moments by using Wick's theorem due to the Gaussian nature of the initial distribution.

IV.C Convergence

In this section we wish to state general results about the convergence properties of the gradient descent dynamics. We begin with presenting a general result about the convergence of the dynamical system.

Theorem 1. *The continuous time system described by Eq. (9) will always converge to some state. The fixed points of the system are any state that is proportional to an eigenstate of H , with the only stable point being the one proportional to the ground state.*

In the following theorem we provide different bounds on the rate of convergence, which, under reasonable conditions, is exponential with time.

Theorem 2. *Given a Hamiltonian H with eigenstates $|E_i\rangle$, eigenvalues E_i , a ground state $|g\rangle$ with energy E_g and a gap Δ . Denoting the energy by $\langle E \rangle$, $\langle E_0 \rangle$ as the initial energy, and the ground state overlap by ψ_g , then for every*

$C > 2$

Case (1): If $\tilde{\psi}_g \neq 0 \forall t$ then

$$|\langle E \rangle - E_g| \leq \begin{cases} \langle E_0 \rangle - E_g e^{-a\Delta t}, & |\langle E \rangle - E_g| \geq \frac{\Delta}{C}, \\ \langle E_0 \rangle \frac{1}{e^{tb} + |\langle E_0 \rangle - E_g| \frac{a}{2b} (e^{tb} - 1)}, & |\langle E \rangle - E_g| \leq \frac{\Delta}{C}, \end{cases}$$

with $a = \frac{\min(\tilde{\psi}_g^2)}{\|\Theta\|C} \frac{1}{\langle g|\Theta^{-1}|g \rangle}$, $b = \frac{C-1}{C^2\|\Theta\|} \max\left(\frac{1}{2^{N+1-2}} \min_{i \geq 1} \left(\frac{|E_i - \Delta/C|}{\langle i|\Theta^{-1}|i \rangle}\right), \Delta \min_i(\Theta_i)\right)$, where $\min(\tilde{\psi}_g^2)$ is a minimum over the entire time of the optimization. Here $\|\cdot\|$ denotes the operator norm.

Case (2): If $|g\rangle$ is an eigenstate of Θ then

$$|\langle E \rangle - E_g| \leq A e^{-\alpha\Delta t} \quad \text{for } |\langle E \rangle - E_g| \geq \frac{\Delta}{C},$$

with $\alpha = \frac{2\langle g|\Theta|g \rangle}{\|\Theta\|C}$, $A = \frac{\|\Theta\|^2 \|H\| - E_g}{\Theta_{\min}^2 \tilde{\psi}_g^2(t=0)}$ and, Θ_{\min}^2 being the smallest eigenvalue of Θ . For $|\langle E \rangle - E_g| \leq \frac{\Delta}{C}$ the bound is the same as in (1).

Case (3): If $[H, \Theta] = 0$ then

$$|\langle E \rangle - E_g| \leq |\langle E_0 \rangle - E_g| \frac{1}{e^{tb} + |\langle E_0 \rangle - E_g| \frac{a}{2b} (e^{tb} - 1)} \quad \text{for } |\langle E \rangle - E_g| \leq \frac{\Delta}{C},$$

with $a = \frac{\Theta_{\min}}{\|\Theta\|C} \tilde{\psi}_g^2(t=0) \langle g|\Theta|g \rangle$ and $b = \frac{C-1}{C^2\|\Theta\|} \min_{i \geq 1} (\langle i|\Theta|i \rangle (E_i - \frac{\Delta}{C}))$. For $|\langle E \rangle - E_g| \geq \frac{\Delta}{C}$ the bound is the same as in (2).

Theorem 2 states that in the most general case, as long as the network optimization process does not dramatically fail (vanishing overlap) then the convergence is exponential with time and dramatically depends on the relationship between the Hamiltonian and the NTK. One can see that the more $|g\rangle$ points in the direction of the principal component of Θ , and the more the other eigenvalues of the NTK are inversely related to the energy spectrum, the faster the bounds will decay to zero with time.

Cases (2) and (3) deal with the specific cases when the ground state and/or other states are also eigenstates of the NTK. In those cases the convergence is guaranteed and the convergence rate for the bounds are better. Using what we know from Sec. III, the third case holds for every Hamiltonian of the form $\sum_S \alpha_S X_S$ with $S \subset \{1, \dots, N\}$ and α_S being real.

It is also important to note that, in accordance with Sec. IV.A, the bounds change below and above the gap. While in the imaginary time Schrödinger equation the convergence scales as $\sim e^{-at}$ with $a = \mathcal{O}(\Delta)$, in the non-trivial NTK case we have $a = \mathcal{O}(\langle g|\Theta|g \rangle \Delta)$ above the gap, depending on the ground state relation with the NTK, while below the gap a is related to an effective gap which depends on the relation between the higher energy eigenstates and the NTK.

It turns out that instead of requiring that $|g\rangle$ will be a ground state of the NTK to achieve better bounds and guarantee convergence, it is enough to require that the variance of the NTK over the ground state will be sufficiently small.

Proposition 2. *If the inequality*

$$\frac{1}{4} \frac{\langle g|\Theta|g \rangle^2}{\langle g|\Theta^2|g \rangle - \langle g|\Theta|g \rangle^2} \geq \frac{\|H\| \|\Theta\| C}{\Delta \psi_g^2(0)}$$

holds, then case (2) in Theorem 2 holds.

One can see that the L.H.S goes to infinity whenever the ground state is an eigenstate of the NTK. The R.H.S will get smaller if the initial overlap with the ground state is larger, which on average depends on the CK expectation value over the ground state. Thus, again, the desirable relation between both kernels and the Hamiltonian is that lower energy states will have larger kernel expectation values.

IV.D Learning Rate

The learning rate is a fundamental hyper-parameter in the context of machine learning. Setting the right learning rate is crucial for convergence. Choosing a learning rate too small will make the convergence very slow, yet choosing a learning rate that is too high will eventually prevent successful convergence. Thus, one usually wishes to choose the largest learning rate while still converging. We provide an upper bound on the learning rate that must be satisfied in order for the process to converge.

Theorem 3. *A necessary condition for the convergence to the ground state is*

$$\Delta t \leq \frac{\langle \psi_0 | \Theta^{-1} | \psi_0 \rangle}{\langle g | \Theta^{-1} | g \rangle} \frac{2}{\left\| \sqrt{\Theta} (H - E_g) \sqrt{\Theta} \right\|}.$$

Although this upper bound cannot be calculated easily, one can see that it is inversely proportional to $\langle g | \Theta^{-1} | g \rangle$, so the more the ground state points in the direction of the principal component of the NTK, the larger the learning rate can be. The operator norm is a bit harder to assess, yet in the highly biased case, when the maximal eigenvalue is much larger than all other eigenvalues, one can write the normalized NTK as $\Theta \approx |\phi\rangle \langle \phi|$, with $|\phi\rangle$ being $|\Theta_0\rangle$ or $|\Theta_1\rangle$ by the results quoted in Sec. III. It follows that $\left\| \sqrt{\Theta} (H - E_g) \sqrt{\Theta} \right\| \approx \langle E \rangle_{|\phi\rangle} - E_g$. Hence, the bound will be higher if the energy expectation value over the principal component of the NTK will be lower, which echoes the same inverse relation between the Hamiltonian and the kernels that is postulated to control the overall performance of the method.

V. The Sign Bias and basis Dependence

V.A Performance Metrics

In light of the above, we define some useful metrics which quantify the compatibility between the Hamiltonian in a given basis and a kernel. We begin with metrics that relate to the bias in the dynamics and initializations toward the ground state,

$$\mathcal{M}(H, \Theta) \equiv \frac{\langle g | \Theta | g \rangle}{\|\Theta\|}, \quad \mathcal{M}(H, K) \equiv \frac{\langle g | K | g \rangle}{\text{Tr}(K)}. \quad (21)$$

The metric $\mathcal{M}(H, \Theta)$ is the dynamical bias toward the ground state, thus providing a measure which is correlated with the convergence rate towards it. $\mathcal{M}(H, K)$ is a rough approximation for the average initial ground state overlap, and should be positively correlated with it. In both cases larger values are desirable.

Since the relations between other energy eigenstates and the kernels are also important for the overall performance, we also consider the additional metrics

$$\mathcal{N}(H, \Theta) \equiv \text{Tr}(H\Theta) - \text{Tr}(H) \text{Tr}(\Theta), \quad \mathcal{N}(H, K) \equiv \frac{\text{Tr}((H - E_g)K)}{\text{Tr}(K)}. \quad (22)$$

$\mathcal{N}(H, K)$ is an approximation for the average initial energy, and should be correlated with it. $\mathcal{N}(H, \Theta)$ is a possible metric for the overall relationship between the Hamiltonian and the NTK, and quantifies how much the desirable inverse correlation between them holds. We thus associate it with the convergence time of the energy to the ground state energy, such that the lower its value the lower the time it takes to reach it. We note that the second term in $\mathcal{N}(H, \Theta)$ is present to account for the invariance of the dynamics under the addition of a multiple of the identity to the Hamiltonian.

We further note that while the CK metrics are derived from an approximation to the average initial values of the ground state overlap and energy, the NTK metrics are less fundamental. We use the NTK metrics to compare different bases while other parameters are kept constant. In other scenarios one might want to use different NTK metrics, which incorporate other factors. For example, in order to distinguish between different models and architectures one will also need to incorporate the dynamics dependence on quantities such as the Hamiltonian and NTK spectra.

V.B The Sign Bias

As was mentioned above, representing the ground state of a Hamiltonian using a neural network is a process that is basis dependent. It can be seen by examining Eq. (9) and noticing that it is not invariant under a change of basis. This is caused by the presence of the non-trivial NTK in the equation, which is the same regardless of the basis we choose to represent the Hamiltonian in. One can also see that the mean initial values such as the energy and the ground state overlap are also not invariant under a change of basis due to the presence of the CK. So although there is no physical meaning to applying a basis transformation to our Hamiltonian, the method is sensitive to the chosen basis. As a result, we will now try to provide some understanding of which basis are preferred by presenting the following results, with derivations given in App. C.

We first show which basis transformations would not effect the performance of the method

Theorem 4. 1. For every unitary U such that $[U, \Theta] = 0$, the solution for the transformed Hamiltonian $\tilde{H} = UHU^\dagger$ is the transformed solution $|\tilde{\psi}\rangle = U|\psi\rangle$, with $|\psi\rangle$ being the solution for the Hamiltonian H .
2. For every unitary U such that $[U, K] = 0$, the average initial values of the energy and ground state overlap are invariant.

The theorem above means that basis transformations that commute with both kernels will yield the same overall performance. By using the known kernels properties in Sec. III it immediately follows that

Corollary 1. Given two Hamiltonians H and \tilde{H} related by a unitary transformation $\tilde{H} = UHU^\dagger$ of the form $U = e^{i\chi}$ with $\chi = \sum_S \alpha_S X_S$, for any real α_S and $S \subset \{1, \dots, N\}$, The solutions are related by $|\psi\rangle = U|\tilde{\psi}\rangle$ with the same average initial conditions. Here $|\psi\rangle, |\tilde{\psi}\rangle$ are the solutions for Eq. (9) under the Hamiltonians H, \tilde{H} respectively.

A specific class of unitary transformation of the form defined above are just X_S with S being any subset of qubits. Their effect is to change the signs of operators involving the Z and Y Pauli matrices in the Hamiltonian, since $-Z = XZX$.

In order to demonstrate the effect of different basis we will focus on Hamiltonians of the form

$$\mathcal{H} = \sum_S \alpha_S X_S + \beta_S Z_S + \gamma_S Y_S, \quad (23)$$

with $\alpha_S, \beta_S, \gamma_S$ being real, S being any subset of qubits, and γ_S being non zero for subsets with even cardinality, in order to make sure the Hamiltonian is real. Although the family is not the most general one can consider, it includes many models of interests including the generalized TFIM, Heisenberg, or the J1-J2 model defined below in Eq. (33).

Corollary 2. For the family of Hamiltonians of the form \mathcal{H} , the average solution is invariant under a unitary change of the signs of β_S and/or γ_S while keeping α_S constant.

The above follows immediately from the fact that altering the signs of β_S and γ_S using a unitary matrix without altering α_S can only be done by applying a unitary of the form X_S . One consequence of this result is that changing the signs over the diagonal using unitary transformation will not affect the performance.

On the other hand, changing the signs of α_S might change the performance based on the results presented in previous sections. Changing the signs of α_S is usually achieved in a unitary fashion using ‘‘sign transformations’’ of the form Z_s , since $ZXZ = -X$.

Proposition 3. Whenever Θ and K are entry-wise positive, for the family of Hamiltonians \mathcal{H} in Eq. (23), the following holds:

- (1) If there is a sign transformation of the form Z_S that will make $\alpha_S \leq 0 \forall S$, then it will minimize $\mathcal{N}(\mathcal{H}, \Theta)$ and $\mathcal{N}(\mathcal{H}, K)$ out of all possible Z_S transformations.
- (2) For $|\gamma_S| \leq |\alpha_S|$, if there is a sign transformation of the form Z_S that will make $\alpha_S \leq 0 \forall S$, then it will maximize $\mathcal{M}(\mathcal{H}, \Theta)$ and $\mathcal{M}(\mathcal{H}, K)$ out of all possible Z_S transformations.
- (3) For $|\gamma_S| \leq |\alpha_S|$, if there is a sign transformation of the form Z_S that will make $\alpha_S \leq 0 \forall S$, then it will maximize the learning rate bound from Sec. IV.D in the large bias approximation as defined in Sec. IV.D, out of all possible Z_S transformations.

Another very common family of Hamiltonians is that of 2-local Hamiltonians, which can be written as

$$H_2 = \sum_\gamma h_i^{(\gamma)} \sigma_i^{(\gamma)} + \sum_{\gamma\delta} \sum_{i,j} J_{i,j}^{(\gamma,\delta)} \sigma_i^{(\gamma)} \sigma_j^{(\delta)}, \quad (24)$$

with $\sigma_i^{(\gamma)} \in \{X_i, Y_i, Z_i\}$ and $i \in \{1, \dots, N\}$. One can also show that

Proposition 4. For two-local Hamiltonians, if there is a sign transformation of the form Z_S that will make $J_{i,j}^{(X,X)}, h_i^{(X)} \leq 0 \forall i, j$, then it will minimize $\mathcal{N}(H_2, \Theta)$ and $\mathcal{N}(H_2, K)$ out of all possible Z_S transformations.

For general Hamiltonians one can also show the following

Proposition 5. For any Hamiltonian H , if Θ and K are entry-wise positive, $\langle g|\Theta|g\rangle$ and $\langle g|K|g\rangle$ are maximized when $\langle \sigma|g\rangle \geq 0, \forall \sigma$ out of all possible signs of $\langle \sigma|g\rangle$ with the same norms.

As mentioned in Sec. III, K is entry-wise positive whenever the activation functions are positive, while Θ is entry-wise positive whenever we have a high bias toward Θ_0 in the NTK spectra, both of which are very common cases.

The results above provide an explanation for why applying a transformation to make the Hamiltonian obey the Marshall-Peierls sign rule before optimizing the network enhanced the performance in previous studies [14, 16, 15]. Such a transformation is a specific case of using a Z_S transformation in order to turn the Hamiltonian into a stoquastic Hamiltonian. Thus the above demonstrates that for the general family of Hamiltonians defined above, if one can make the Hamiltonian stoquastic using a Z_S transformation, then it will tend to improve the performance of the optimization, making the stoquastic form preferred whenever it is attainable.

More generally, it was shown empirically that stoquastic Hamiltonians are easier for NQS ground state optimizations [15, 13], as compared to highly non-stoquastic Hamiltonians. One of the reasons for this phenomenon is the fact that for a lot of common ANN architectures, the kernels will be highly biased toward their principal component. From the kernels property in Eq. (12), the principal component always have a simple sign structure, and in most common cases, it is the state $|+\rangle = \frac{1}{2^{N/2}} \sum_{\sigma} |\sigma\rangle$ which is “in the middle” of the positive cone. Since stoquastic Hamiltonians always have a positive ground state, $\langle g|\sigma\rangle \geq 0$, the bias is compatible with their ground states, in the sense that the kernel expectation values over the ground state will be large compare to non-stoquastic Hamiltonians. One can see that by considering the extremely biased case toward the $|+\rangle$ state, where $\mathcal{M}(H, \Theta) \propto \langle g|\Theta|g\rangle \approx (\sum_{\sigma} \langle \sigma|g\rangle)^2$. Thus, in general ground state with a uniform sign structure will have larger kernel expectation then a ground state with a highly non-uniform signs.

On top of that, stoquastic Hamiltonians will yield low values for $\mathcal{N}(H, \Theta)$ and $\mathcal{N}(H, K)$, meaning that they will be strongly compatible with the kernels, in the sense that lower energy states will have higher kernels expectation values. One can see that for example by considering the most general form of two-local Hamiltonians in Eq. (24), which are the most common local Hamiltonians in practical settings. For such Hamiltonians

$$\mathcal{N}(H_2, \Theta) = \sum_{i,j} J_{i,j}^{(X,X)} \alpha_2 + h_i^{(X)} \alpha_1$$

where we assumed that $\text{Tr}(H) = 0, \|H\|_F = \|\Theta\|_F$ W.L.G. α_1, α_2 depend on Θ , and whenever there is a significant bias toward $|+\rangle$ they are both positive. A necessary condition for a 2-local Hamiltonians to be stoquastic is that $J_{i,j}^{(X,X)}, J_{i,j}^{(X,I)}, J_{i,j}^{(X,J)}$ will all be negative. And a negative value of those coefficients will in general produce a low value for $\mathcal{N}(H, \Theta)$ compared to a highly non-stoquastic Hamiltonians with highly non-uniform signs for those coefficients.

Even in the most general case, without assuming anything about the kernels, using the weak bias property in Eq. (12), there will always be some bias toward states with less “complex” sign structures. As mentioned, the kernels eigenstates are the states $|s\rangle$ with s being a string of $+$ and $-$. The kernels spectra decomposes into sectors, each one of which is a subspace spanned by the states $|s\rangle$ with a specific number of $+$ signs. Each sector has a unique complexity as was defined in Sec. III and [33], which is the number of Hilbert space dimensions that the state oscillates in. The weak bias property of every NTK and CK states that there will always be some bias toward a “simple” subspace with complexity 0 or 1. Thus, ground states which have their most significant component in low complexity sectors will be more aligned with the bias, while highly “oscillating” ground states will be much less aligned, rendering them harder to learn. Due to the exponential growth of Hilbert space, the bias toward the principal component will grow exponentially with the system size.

V.C Basis Optimization

One can utilize the relations between the metrics $\mathcal{N}(H, \Theta)$ and $\mathcal{N}(H, K)$ and the overall performance in order to find the local basis most suitable for the ANN at hand. In the case of 2-local Hamiltonians, every local basis transformation, described by a set of unitary matrices $U_i \in SU(2), i \in \{1, \dots, N\}$, such that $\tilde{H} = UHU^\dagger$ with $U = \otimes_i^N U_i$, corresponds to a set of orthogonal matrices $O_i \in O(3)$, that transform the Hamiltonian coefficients as [29]

$$\tilde{h}_i^{(\gamma)} = \sum_{\delta} O_i^{(\gamma,\delta)} h_i^{(\delta)}, \quad \tilde{J}_{i,j}^{(\gamma,\delta)} = \sum_{\alpha,\beta} O_i^{(\gamma,\alpha)} J_{i,j}^{(\alpha,\beta)} O_j^{(\beta,\delta)}. \quad (25)$$

For example, one can then try to optimize $\mathcal{N}(\tilde{H}, K)$ over these orthogonal matrices. Since under a basis transformation the trace is preserved, ones has

$$\mathcal{N}(\tilde{H}, K) = \text{Tr}(\tilde{H}K) = k_2 \sum_{i,\delta} O_i^{(X,\delta)} h_i^{(\delta)} + k_1 \sum_{i,j,\alpha,\beta} O_j^{(X,\alpha)} J_{i,j}^{(\alpha,\beta)} O_j^{(\beta,X)}, \quad (26)$$

with $k_1 \equiv \text{Tr}(X_1 K)$ and $k_2 \equiv \text{Tr}(X_1 X_2 K)$, which depends on the network. This optimization is not easy in general. In the translationally invariant case one can restrict oneself to a uniform transformation, meaning that $O_i \equiv O$, which reduces the number of variables to a constant. Consider for example the TFIM in Eq. (11), and consider transformations which will render the transformed Hamiltonian real for the sake of simplicity. Then the transformation takes place in the XZ plane, meaning that $O \in O(2)$. One can further verify that in our case it is enough to consider $O \in SO(2)$, which is parameterized by a single parameter θ . Carrying out the calculation one obtains

$$\mathcal{N}(\tilde{H}, K) = -k_2 J \sin^2(\theta) - k_1 h N \cos(\theta), \quad (27)$$

with J being the number of edges over the interactions graph. Optimizing this expression in term of θ , one finds that the optimal value of $\mathcal{N}(\tilde{H}, K)$ is $\min\left\{-k_2 J - \frac{k_2 N^2 h^2}{4 K_2 J}, -k_1 N h, k_1 N h\right\}$, which corresponds to $\theta = \arccos\left(-\frac{h k_1 N}{2 k_2 J}\right)$, $\theta = 0$, $\theta = \frac{\pi}{2}$, respectively. k_1 and k_2 can be approximated in the extremely biased regime when the bias is toward $|+\rangle$ such that $k_1 \approx k_2$. In other cases, for common activation functions and architectures one can use various method to evaluate them approximately or extrapolate from small system sizes [18, 20, 33, 35].

VI. Numerical Results

We demonstrate the ideas presented above in numerical experiments in the infinite limit. Specifically, we will show that the metrics $\mathcal{M}(H, \Theta)$, $\mathcal{N}(H, \Theta)$, $\mathcal{M}(H, K)$, and $\mathcal{N}(H, K)$ are indeed correlated, respectively, with the convergence time of the network to the ground state, their ground state energy, and the initial values of both these quantities.

VI.A NTK vs. Convergence Time

$\mathcal{N}(H, \Theta)$ is a version of the inner product between the Hamiltonian and NTK, and thus provides an a-priori metric about the overall relationship between the Hamiltonian and NTK spectra and eigenstates. As conjectured, the lower it is, the faster the energy will decrease overall, due to the bias toward lower energy eigenstates in general.

$\mathcal{M}(H, \Theta)$ is proportional to the expectation value of the NTK over the ground state, so it provides a measure for the bias of the optimization toward to ground state, as compared to the principal component. It is important to note that $\mathcal{N}(H, \Theta)$ can be small, indicating that the bias will be compatible with lowering the overall energy, while $\mathcal{M}(H, \Theta)$ is also small, so obtaining a low energy state will be easy, yet obtaining the actual ground state will be hard. As noted before, these metrics are only sensible when one uses them to compare different bases, while keeping the initial conditions the same.

In this section we will consider different models and different architectures under a local basis transformation, which is determined by a single parameter in a similar fashion to Sec. V.C. In order to eliminate the influence of the initial conditions determined on average by the CK, we use the initial uniform superposition

$$|\psi_0\rangle = \sum_i |E_i\rangle, \quad (28)$$

with $|E_i\rangle$ being the eigenstates of the Hamiltonian.

In Fig. 2 we consider the noninteracting Hamiltonian

$$H_{\text{local}} = - \sum_i X_i, \quad (29)$$

which under local basis rotation assumes the form

$$H_{\text{local}} = \sum -\cos(\theta) X - \sin(\theta) Z. \quad (30)$$

Following Sec. V.C we expect that the smaller θ is, the faster the NQS will converge to the ground state; As can be seen from the results, this is indeed the case. We also see that the metric $\mathcal{M}(H, \Theta)$ is indeed positively correlated with the convergence time.

We use the same metric in Fig. 2 for the TFIM model in Eq. (11), with $h_i = 2$. Under local basis rotation, from the analysis in Sec. IV.C we expect the fastest convergence to occur when $\theta = 0$, which is indeed the case. This can be understood from the more general analysis, since this is the case where the negative off diagonal elements are most dominant.

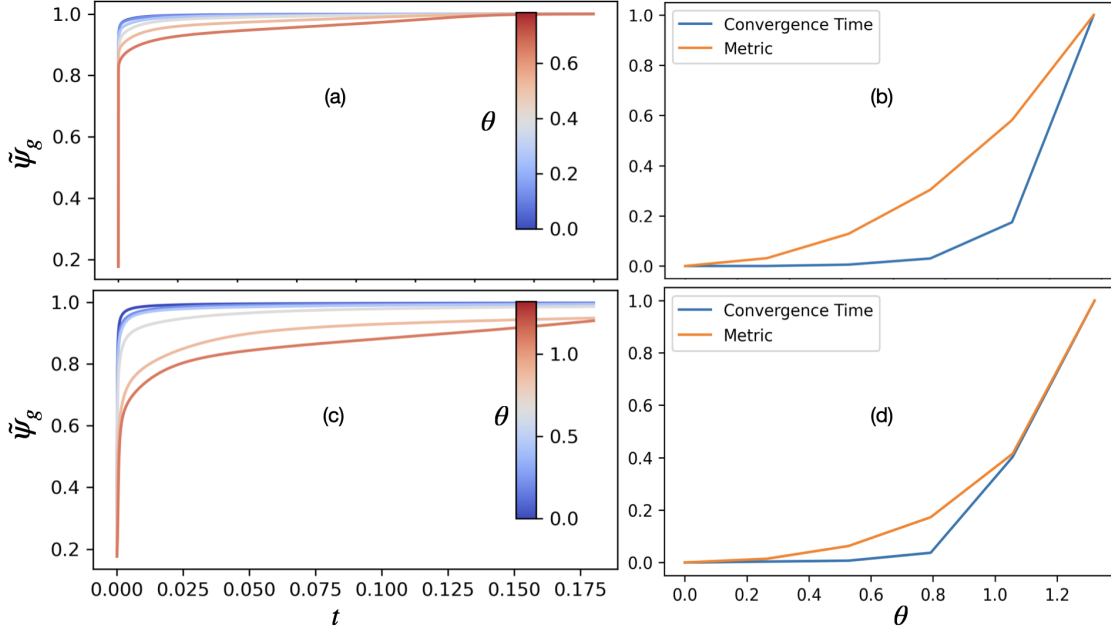


Figure 2: (a) The ground state overlap as a function of time for H_{TFIM} with varying θ . (b) The convergence time, which is the time it takes for the overlap to reach a fixed threshold $\epsilon = 0.95$ and the metric $\mathcal{M}(H, \Theta)$ as a function of θ . (c) The ground state overlap as a function of time for H_{local} for $\theta \in [0, \frac{\pi}{2}]$. (d) The convergence time and the metric $\mathcal{M}(H, \Theta)$ plotted as a function of θ . Both networks have one hidden layer and a ReLU activation. Metrics and convergence times are normalized to the range $[0, 1]$.

We also examine if the metric $\mathcal{N}(H, \Theta)$ is positively correlated with the convergence time of the energy to the ground state energy. We first examine this relationship for the Heisenberg model with a transverse field,

$$H_{\text{Heis}} = \sum_{\langle i,j \rangle} \vec{\sigma}_i \cdot \vec{\sigma}_j - h \sum_i X_i, \quad (31)$$

with $h = 1$. We note that the transverse field is introduced since otherwise the Hamiltonian would be invariant under uniform local basis transformations. Due to the symmetry of the coupling term we expect to get similar results to the uncoupled chain, such that the minima will occur at $\theta = 0$. As can be seen in Fig. 3, this is indeed the case. One can also see that the metric $\mathcal{N}(H, \Theta)$ is indeed positively correlated with the convergence time. We further demonstrate this relation for the XYZ Hamiltonian

$$H_{\text{XYZ}} = \sum_{\langle i,j \rangle} \alpha X_i X_j + \beta Z_i Z_j + \gamma Y_i Y_j, \quad (32)$$

with $\alpha = -2, \beta = -1, \gamma = -0.5$. Again one can observe in Fig. 3 that the metric $\mathcal{N}(H, \Theta)$ is highly correlated with the convergence time for the energy expectation over the NQS.

In Fig. 4 we provide the results of additional benchmarks with different models and architectures, which all seem to indicate a strong relationship between the metrics and the corresponding convergence time.

Beyond the general correlation between the metrics and the convergence time, one can see that in all of the models we examined, local minima for the convergence time are aligned with the local minima for the metrics. All of those local minima occur when the negative off diagonal terms are the most dominant relative to other bases. Further details are provided in App. D.

VI.B CK vs. Initial Averages

As was mentioned in Sec. III.B, the CK is just the covariance matrix of the gaussian distribution of the initial unnormalized states. The metrics $\mathcal{N}(H, K)$ and $\mathcal{M}(H, K)$ are just the large- N approximations to the average initial energy and ground state overlap, respectively.

In Fig. 5 we plot the averages and their corresponding metrics in several cases. Similarly to the previous subsection, we use the uncoupled Hamiltonian as defined in Eq. (30) under local unitary basis transformation. We

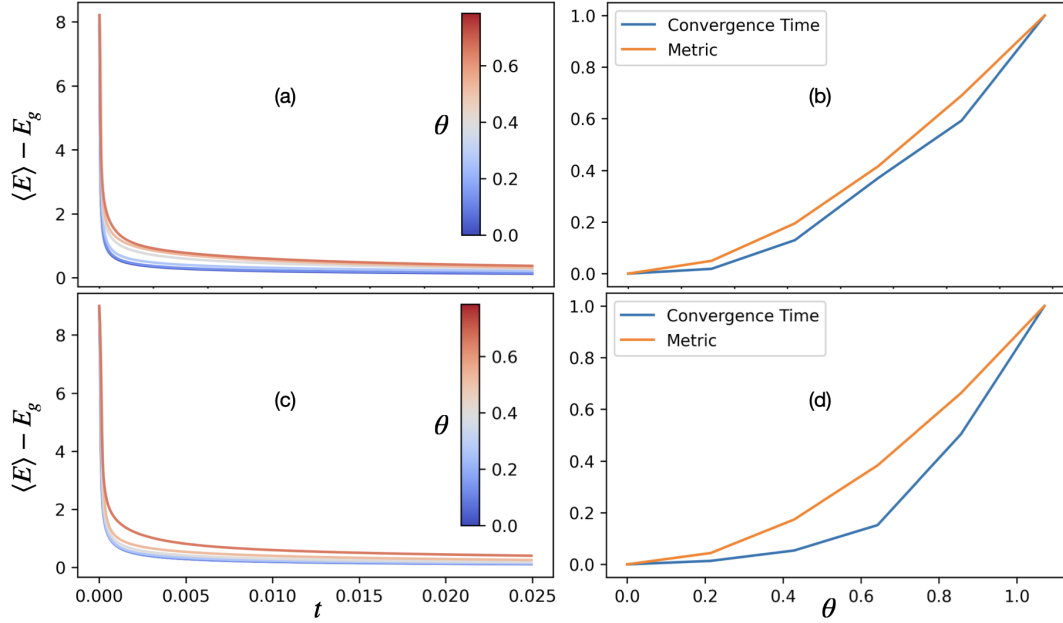


Figure 3: (a) The energy as a function of time for H_{XYZ} for different local basis. (b) The average convergence time and the metric $\mathcal{N}(H, \Theta)$ as a function of θ normalized to the range $[0, 1]$. (c) The energy as a function of time for H_{Heis} for different local basis. (d) the average convergence time and the $\mathcal{N}(H, \Theta)$ as a function of θ normalized to the range $[0, 1]$. Both networks consist of one hidden layer with ReLU activation. Metrics and convergence times are normalized to the range $[0, 1]$.

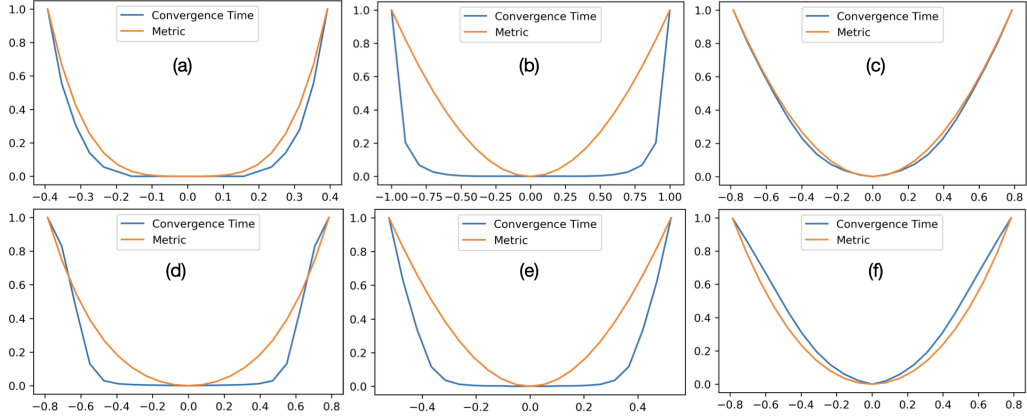


Figure 4: (a) Ground state overlap convergence time and $\mathcal{M}(H, \Theta)$ for H_{local} with one hidden layer and tanh activation. Energy convergence time and the metric $\mathcal{N}(H, \Theta)$ for H_{Heis} with (b) one hidden layer and erf activation, and (c) two hidden layers with ReLU activation. (d) Ground state overlap convergence time and $\mathcal{M}(H, \Theta)$ for H_{TFIM} with one hidden layer and erf activation. (e) Energy convergence time and the metric $\mathcal{N}(H, \Theta)$ for H_{XYZ} with one hidden layer and sigmoid activation function. (f) Energy convergence time and the metric $\mathcal{N}(H, \Theta)$ for H_{TFIM} with two hidden layers and ReLU activation function. Metrics and convergence times are normalized to the range $[0, 1]$

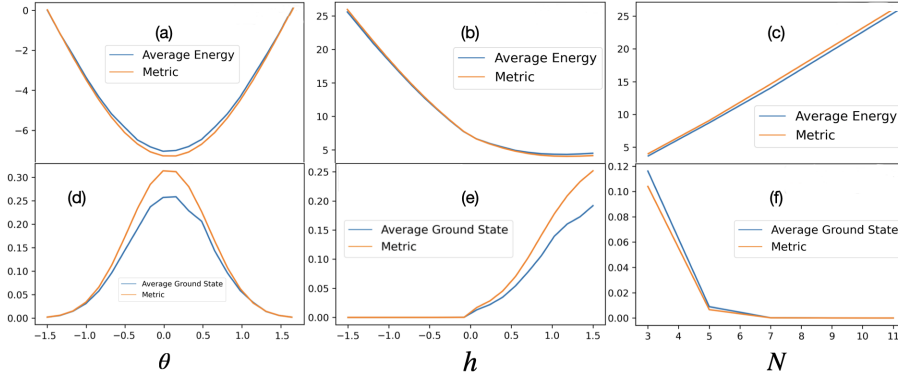


Figure 5: (a,b,c) Average initial energy and (d,e,f) ground state overlap together with their corresponding metrics $\mathcal{N}(H, K)$ and $\mathcal{M}(H, K)$, averaged over 10^3 samples. (a,d) The model H_θ with $\theta \in [0, \pi]$, where we omitted the E_g term from $\mathcal{N}(H, K)$ due to it being independent of θ . (b,e) The TFIM as a function of $h \in [-1.5, 1.5]$, where negative values of h correspond to positive off diagonal elements in the Hamiltonian and vice versa. (c,f) The J_1 - J_2 model at with $J_1/J_2 = 0.5$ as a function of N . For all of the above we used one hidden layer and ReLU activation function.

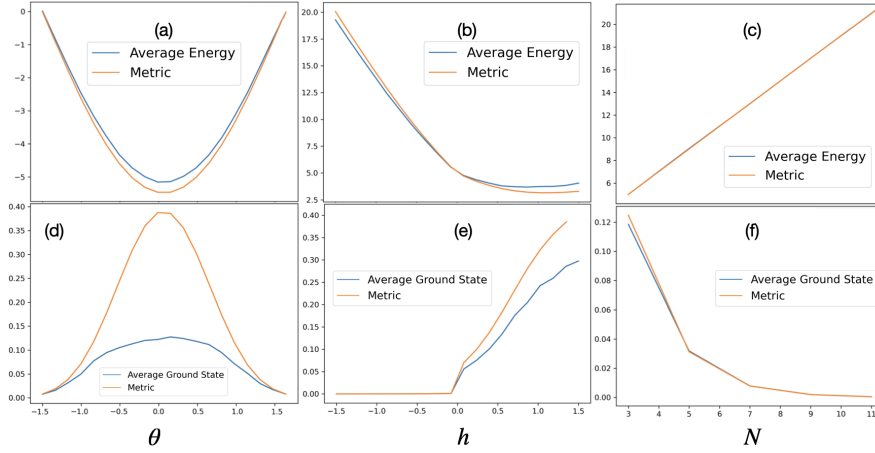


Figure 6: (a,b,c) Average initial energy and (d,e,f) ground state overlap with their corresponding metrics. (a,d) H_θ with $\theta \in [0, \pi]$, with tanh activation function and one hidden layer. (b,e) H_{TFIM} with $h \in [-1.5, 1.5]$, with two layers and ReLU activation. (c,f): H_{Ising} with sigmoid activation function.

also examine the dependence over a model parameter such as the strength of the transverse field in the case of the TFIM. We observe that the more the negative off-diagonal elements are dominant, the better the metrics and averages. We also note that there is a crucial difference between negative and positive off diagonal elements in the initial ground state overlap. Finally we use the 1D J_1 - J_2 model,

$$H_{J_1-J_2} \equiv J_1 \sum_{\langle i, j \rangle} \vec{\sigma}_i \vec{\sigma}_j + J_2 \sum_{\langle\langle i, j \rangle\rangle} \vec{\sigma}_i \vec{\sigma}_j, \quad (33)$$

with $\langle\langle i, j \rangle\rangle$ indicating next nearest neighbors, with $J_1 = 1$ and $J_2 = \frac{1}{2}$. One can see that the ground state overlap prediction is quite accurate, and that it displays a rapid decrease as a function of N . Although we use a 1D example we can already see how the metrics can predict the hardness of trying to simulate the J_1 - J_2 model using ANN.

In Fig. 6 we add further benchmarks. One can see that in some cases there can be large deviations between the metric and the actual average, due to the rough estimation the metrics were derived from. Nonetheless, their trends perfectly match. This can be used for the purpose of comparing different parameters, bases, or architectures.

VII. Stochastic Reconfiguration

The non-triviality of the NTK arises from the fact that the gradient flow is performed in parameter space. A method known more generally as natural gradient and in our specific context as Stochastic Reconfiguration (SR) [36, 37, 23] attempts to mimic a gradient flow in the wavefunction space (which in our case is just the Hilbert space). It is usually achieved by a modification of the parameter update such that

$$\frac{d\theta_i}{dt} = \sum_j (J^T J + \epsilon I)^{-1}_{ij} \frac{d\mathcal{L}}{d\theta_j}, \quad (34)$$

with $J_{\sigma i} = \frac{\partial \psi_\sigma}{\partial \theta_i}$. Can it alleviate the kernel bias discussed above? Using the chain rule we get

$$\frac{d|\psi\rangle}{dt} = \frac{1}{\langle\psi|\psi\rangle} (I + \epsilon\Theta^{-1})^{-1} (\langle E\rangle - H) |\psi\rangle, \quad (35)$$

which for a sufficiently small ϵ , in the limit of infinite width, is indeed the imaginary time Schrödinger equation. Although it might seem as a remedy to the kernel bias, it is important to notice several points. The first is that the initialization is still governed by the CK, and biased in the same manner, so using the usual initialization strategies will produce a poor initial overlap with the ground state when the CK expectation value over the ground state is low.

Another thing that one can notice from the equation above, is that it is the same as Eq. (9), with $\Theta_{\text{eff}} = (I + \epsilon\Theta^{-1})^{-1} \approx I - \epsilon\Theta^{-1}$. One can then see that in order to guarantee that the resulting equation will mimic the imaginary time Schrödinger equation one needs to have

$$\epsilon \ll \Theta_{\min} \quad (36)$$

with Θ_{\min} being the minimal eigenvalue of Θ . We note that using the results listed in Sec. III, Θ_{\min} decays as $\sim \frac{1}{2^{N^2}}$, so one will need a very small ϵ to fully mimic the imaginary time dynamics. If ϵ is not small enough, then the effective NTK affect can be non-trivial and might induce a significant bias. Following the analysis presented before, in order for the dynamical bias to be aligned with the ground state, $\langle g|\Theta_{\text{eff}}|g\rangle \approx 1 - \epsilon\langle g|\Theta^{-1}|g\rangle$ should come close to unity as much as possible, so $\langle g|\Theta^{-1}|g\rangle$ should be small as possible, similar to the case without the SR method.

It is also important to note that these observations should also be weighted against the fact that since the application of the SR method requires a matrix inversion, each parameter update requires $\mathcal{O}(p^3)$ operations with p being the number of parameters, so in general it is mostly applicable to small systems [23].

VIII. General Ansätze

In this section, we discuss how our approach for the study of the possible existence of a sign bias, or, more generally, the basis dependence, might relate to other ansatz that are optimized under gradient descent.

For a general ansätze, the dynamics would be governed by the equation

$$\frac{d|\psi\rangle}{dt} = \frac{1}{\langle\psi|\psi\rangle} \Theta_t (\langle E\rangle - H) |\psi\rangle, \quad (37)$$

with the NTK being potentially time dependent now, and where the ansätze might not be able to represent every state in Hilbert space.

We begin by asking what are the criteria for the performance of the ansätze to be invariant under some change of basis, represented by a unitary transformation U . We denote the solution the equation above with H by $\psi_\sigma(\theta(t))$ and the solution for the transformed Hamiltonian $\tilde{H} = UH U^\dagger$ by $\psi_\sigma(\tilde{\theta}(t))$, with θ and $\tilde{\theta}$ being the parameters of the two solutions.

1. The initial average (over the distribution of the function parameters) of the every function of interest, e.g., the energy expectation value or the ground state overlap should be invariant under U . For a general Hamiltonian this would require

$$p_0(\psi_\sigma) = p_0 \left(\sum_{\sigma'} U_{\sigma\sigma'} \psi_{\sigma'} \right)$$

with p_0 being the initial distribution of the wavefunction.

2. For all t there is a set of parameters $\tilde{\theta}$ such that $\psi_\sigma(\tilde{\theta}(t)) = \sum_{\sigma'} U_{\sigma\sigma'} \psi_\sigma(\theta(t))$.

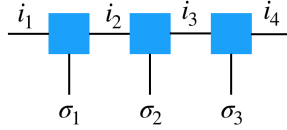
In general, verifying that these criteria are obeyed is not easy. For infinite NQS, the second criteria is trivial, and the first criterion reduces to the much simpler criterion that the NTK and CK will commute with U as stated on Sec. III due to the emergence of gaussian distribution for the initial state and the convergence of the NTK to its mean initial value. In the following subsection we show a very well known ansätze that can be seen to satisfy those criteria for every local unitary transformation

VIII.A Matrix Product States are Local-Basis Unbiased

Let us consider the most elementary tensor network, the Matrix Product States (MPS), which is defined algebraically as

$$\psi_\sigma = \sum_{i_1, \dots, i_N} \left(\prod_n A_{i_n, i_{n+1}}^{(\sigma_n)} \right), \quad (38)$$

for a system of N spins, with each $A_{i_n, i_{n+1}}^{(\sigma_n)}$ being an order 3 tensor. The upper index $\sigma_n \in \{-1, 1\}$ corresponds to one of the physical spins, while the indices $i_n \in \{1, \dots, \chi\}$ are virtual (dummy) indices to be summed over. For simplicity we will consider periodic boundary conditions where $i_1 = i_N$. MPSs are usually represented graphically using vertices and edges as follows



with each blue square with 3 black legs corresponding to a tensor $A_{i_n, i_{n+1}}^{(\sigma_n)}$. The capacity of the ansatz is controlled mainly by the geometry of the network and the virtual bond dimension χ .

Lets us begin by showing the first criterion is met for local unitaries. Usually the matrices $A^{(\sigma_n)}$ are drawn i.i.d, from distributions such as the Haar measure, matrix normal distributions and entrywise normal distributions. If that is the case then

$$P(\psi_\sigma) = \prod_n P\left(A^{(\sigma_n)}\right)$$

due to the i.i.d property. Thus, for local unitaries the first criterion amounts to

$$p\left(A^{(\sigma_n)}\right) = p\left(\sum_{\sigma'_n} U_{\sigma_n \sigma'_n} A^{(\sigma'_n)}\right).$$

This criteria can easily be seen to be met whenever

$$p\left(A^{(\sigma_n)}\right) = p\left(\sum_{\sigma_n} A^{(\sigma_n)} A^{(\sigma_n)T}\right)$$

,which is met for the Haar measure, matrix normal distribution with identity covariance, entrywise normal distribution, and every other distribution for the matrix distribution which is invariant under the application of a unitary.

The second criterion is immediate for every local unitary transformation. Indeed, if we apply a local unitary U on a spin n , the MPS will transform into another MPS with the same bond dimension and local matrix $\tilde{A}^{(\sigma_n)} = \sum_{\sigma'_n} U_{\sigma_n \sigma'_n} A^{(\sigma'_n)}$. Hence, MPSs are locally unbiased and will not suffer from a sign bias that can be solved by local change of basis.

In the case that the MPS is overparameterized, i.e., that χ is large enough such that it can represent every N spins wave function, the first criterion is met for every unitary U , even a non-local one, under mild conditions. Considering Eq. (38), since there are a total of $N\chi$ product terms in the sum, the wave function ψ_σ will be distributed according to a normal distribution by virtue of the central limit theorem. For a fixed N , the deviation from the central limit theorem will scale with the bond dimension as $\chi^{-N/2}$ in the case that each $A^{(\sigma_n)}$ is entrywise

i.i.d, and at least as $\chi^{-1/2}$ if we allow correlations. The covariance matrix for the normal distribution is analogous to the CK and is given by

$$K = \langle \psi_\sigma(0) \psi_{\sigma'}(0) \rangle.$$

using Eq. (38) and the independence we obtain

$$\begin{aligned} \langle \psi_\sigma(0) \psi_{\sigma'}(0) \rangle &= \left\langle \sum_{i_1, \dots, i_N} \left(\prod_n A_{i_n, i_{n+1}}^{(\sigma_n)} \right) \sum_{i_1, \dots, i_N} \left(\prod_n A_{i_n, i_{n+1}}^{(\sigma'_n)} \right) \right\rangle \\ &= \sum_{i_1, \dots, i_N, i'_1, \dots, i'_N} \prod_n \langle A_{i_n, i_{n+1}}^{(\sigma_n)} A_{i'_n, i'_{n+1}}^{(\sigma'_n)} \rangle = \sum_{i_1, \dots, i_N, i'_1, \dots, i'_N} \prod_n \langle A_{i_n, i_{n+1}}^{(\sigma_n)} A_{i'_n, i'_{n+1}}^{(\sigma'_n)} \rangle \delta_{\sigma_n, \sigma'_n}, \end{aligned}$$

where in the last equality we used the i.i.d property of the matrices $A^{(\sigma_n)}$. Finally we get

$$\langle \psi_\sigma(0) \psi_{\sigma'}(0) \rangle = \left(\sum_{i_1, \dots, i_N, i'_1, \dots, i'_N} \prod_n \langle A_{i_n, i_{n+1}}^{(\sigma_n)} A_{i'_n, i'_{n+1}}^{(\sigma_n)} \rangle \right) \delta_{\sigma, \sigma'} \propto \delta_{\sigma, \sigma'}.$$

Since the CK is proportional to the identity it will commute with every unitary U . The second criterion is trivially obeyed in the overparametrized limit.

IX. Conclusions and Future Outlook

In this work we explored how the interplay between a neural network architecture and a Hamiltonian affects the success of learning the Hamiltonian ground state. Building upon recent developments in neural network theory, we have used an infinite width limit which provides twofold simplification; First, it provided mathematical simplicity that allowed the study of the network initialization and dynamical properties in a more tractable manner. Second, it absolved us from going into the separate discussion of the network capacity. In this spirit we also avoided going into the use of Monte Carlo techniques. Although not practical, we could use these settings to reveal the more fundamental obstacles that this method faces, which cannot be alleviated by increased computational resources.

Using two known quantities characterizing the network in this limit, the NTK and the CK, we have derived several results, from which we could come up with simple criteria quantifying the desired relationship between them and the Hamiltonian, criteria which are correlated with the success of the method, namely that the lower the energy of a Hamiltonian eigenstate, the larger its kernel expectation should be. This is a manifestation of a general feature of neural network, which are known to have implicit biases [34, 33]. We quantified that property using several metrics and showed its relationship to the network convergence rates and initial state properties, both theoretically and numerically.

Using these metrics and theorems, we demonstrated that the overall performance of the method depends both on the basis the Hamiltonian is presented in and its basis invariant spectrum. Although some models will be harder than others due to their spectral properties, for example due to their smaller gap, which is true for almost every numerical method, the NN method is also very sensitive to the chosen basis. Using the tools developed throughout the paper we were able to characterize which basis transformation can influence the performance, and demonstrated how and why common strategies to choose the basis, such as the Marshall-Peierls sign rule, enhanced performance [14, 16, 15]. We were also able to elucidate the affect of basis dependent properties of the Hamiltonian, such as its “stoquasticity” and the sign structure of its ground-state. This in turn provided a fundamental explanation to an empirical observation, that there is a sort of a manifestation of the sign problem for ANNs, namely, that stoquastic Hamiltonians are easier than non-stoquastic ones [15, 13]. By characterizing and quantifying the basis dependence we also open a new study direction toward developing methods to find a more suitable basis or even an optimal one. One may then incorporate those idea as a sub-routine before optimizing the network.

Given a Hamiltonian, we also demonstrated how the metrics provided can predict the overall performance based on the network architecture and its hyper parameters. Although we limited ourselves to a rather simple feed-forward network, one can apply the same techniques to more complicated architectures, recalling the NTK and CK limits apply to most common ones, such as convolutional neural networks [19, 38], recurrent neural networks [39, 35], transformers [40] and others [41]. This in turns might provide a pathway to understanding what are the desirable characteristics of a neural network architecture when trying to find the ground state of a given Hamiltonian.

We also mention that we focused on metrics that provide a more “macroscopic” overall description of the relationship between a Hamiltonian and the kernels. This allowed us to address general questions about general

Hamiltonians. Yet, when one considers a specific model that one wished to study using a specific ANN, it can be more beneficial to take a more fine grained approach and define metrics which are relevant to the task at hand in order to fully describe the relationship between the specific Hamiltonian and architecture and its influence on the performance. We leave this as a direction for future work.

While we mainly explored the initialization and dynamics for neural networks, some of the idea discusses in the paper might be useful for other ansätze, as we briefly demonstrated in VIII. As we showed, the sign bias might not manifest itself for some ansätze such as MPSs and further investigation using similar techniques might shed a light about other structural differences between different ansätze. A future study could focus on how the metrics we proposed might vary between different ansätze and look into their dynamics in the case of a dynamical NTK.

To summarize, the techniques developed and used in this paper provide a way to study both theoretical and practical questions regarding NQS methods for many-body Hamiltonians. It remains to be seen if and how similar techniques can be applied to other variational methods, and how other concepts we disregarded throughout the paper, such as representability and stochastic optimization strategies, influence the general conclusions drawn here when a particular setting is considered.

We would like to thank Y. Bar Sinai, G. Cohen, S. Gazit, and Z. Ringel for useful discussions. Support by the Israel Science Foundation (ISF) and the Directorate for Defense Research and Development (DDR&D) Grant No. 3427/21, the ISF grant No. 1113/23, and the US-Israel Binational Science Foundation (BSF) Grant No. 2020072 is gratefully acknowledged.

Appendix

App. A Applicability of the NTK limit

It is stated in [42] that the NTK limit, or the lazy training regime as it is often referred to, is guaranteed to hold whenever

$$\frac{\mathcal{L}(\theta_0)}{\|\nabla\mathcal{L}(\theta_0)\|} \frac{\|D^2f(\theta_0)\|}{\|Df(\theta_0)\|^2} \ll 1,$$

with $\mathcal{L}(\theta_0)$ being the loss function at initialization, ∇ denoting the natural gradient, i.e, the gradient with respect to the outputs of the network, D denoting the differential of the outputs with respect to the parameters, and $\|\cdot\|$ denoting the vector or operator norm depending on the context. It is also assumed without the loss of generality that the loss is always positive. For the energy loss function the criterion above amounts to

$$\frac{\sqrt{\langle\psi_0|\psi_0\rangle}}{\sqrt{\langle H^2\rangle_0/\langle H\rangle_0^2-1}} \frac{\|D^2\psi(\theta_0)\|}{\|D\psi(\theta_0)\|^2} \ll 1,$$

with $\langle\cdot\rangle_0 \equiv \frac{\langle\psi_0|\cdot|\psi_0\rangle}{\langle\psi_0|\psi_0\rangle}$ being the average over the initial state $|\psi_0\rangle$. The term $\langle H^2\rangle_0/\langle H\rangle_0^2-1$ approaches some limiting value in the infinite width limit, which on average depends on the relationship between the CK and the specific Hamiltonian. This value is zero if and only if the initial state happens to be an eigenstate of the Hamiltonian, which is a zero measure event. The term $\langle\psi_0|\psi_0\rangle$ approaches the value $\text{Tr}(K)$ with K being the CK when the width approaches infinity. As long as one uses the NTK initialization scheme, as mentioned in [42, 17], this term approaches a non zero value. These two terms, hence their ratio, do not scale with the number of hidden neurons. On the other hand, the term $\frac{\|D^2\psi(\theta_0)\|}{\|D\psi(\theta_0)\|^2}$ does scales with the number of hidden neurons N as $\mathcal{O}(N^{-1/2})$, as mentioned in [42, 17]. Thus, the infinite width limit becomes valid when

$$N^{-1/2} \ll 1.$$

It is also worth mentioning that contrary to the case of mean-squared error loss, where one can approach the lazy training regime by rescaling the output of the neural network by a factor $\alpha \gg 1$ [42], the normalization of the energy loss is such that one cannot approach the lazy training regime by rescaling; indeed, it is easy to see that the above criterion remains invariant under the transformation $\psi \rightarrow \alpha\psi$.

App. B Proofs for Sec. IV

Proof. Proposition 1: The proof follows immediately from the implicit solution to Eq. (9)

$$|\psi\rangle = \exp[\Theta(f - Hh)]|\psi_0\rangle,$$

with $f \equiv \int_0^t \frac{\langle E \rangle}{\langle \psi | \psi \rangle} dt'$, $h \equiv \int_0^t \frac{1}{\langle \psi | \psi \rangle} dt'$ and $|\psi_0\rangle$ being the initial state. Since $[H, \Theta] = 0$ we have that

$$\frac{\tilde{\psi}_j}{\tilde{\psi}_i} = \exp[\Theta_j (f - E_g h) - \Theta_i (f - E_i h)] \frac{\tilde{\psi}_j(t=0)}{\tilde{\psi}_i(t=0)}.$$

Taking the square and differentiating with respect to time we get the result. \square

Lemma 1. *Given a $d \times d$ positive definite matrix A with eigenvalues a_i , $a_0 = 0$ and constrained Frobenius norm $0 < \|A\|_F < C$, the maximal gap $\alpha_* = \max_{\alpha_i} \min_{i>0} \{\alpha_i\}$ occurs when $\alpha_i = \frac{C}{\sqrt{d-1}}$.*

Proof. Defining the function $\sum e^{-\alpha_i t} + \lambda \sum_i \alpha_i^2$, one can notice that as $t \rightarrow \infty$ the first term is dominated by $1 + e^{-\min_{i>0} \{\alpha_i\} t}$, so we wish to minimize this function. Differentiating with respect to α_i for $i > 0$ we get $\alpha_i = \frac{t}{\lambda} e^{-t\alpha_i}$. Using the constraint we obtain $\lambda^2 \geq \frac{t^2}{C^2} \sum_{i>0} e^{-2t\alpha_i}$. Thus, $\alpha_i \leq C \frac{e^{-t\alpha_i}}{\sqrt{\sum_{i>0} e^{-2t\alpha_i}}}$. Assume that $\alpha_k \equiv \min\{\alpha_i\}$ satisfies $\alpha_k < \alpha_i$ for $i \neq k$; then $\alpha_i \leq 0$ for all $i \neq k$, which is a contradiction to the assumption that α_k is minimal unless $\alpha_i = 0 \forall i$. The only other possibility is that α_i is constant for all $i > 0$, which gives $\alpha_* \leq \frac{C}{\sqrt{d-1}}$. Maximizing α_* yields the result. \square

Lemma 2. *Given an Hamiltonian H , the maximal gap of the matrix $\tilde{H} = \sqrt{\Theta}(H - E_g)\sqrt{\Theta}$ under the constraint that $\|\Theta\|_F < C$ for some finite C , occurs if and only if $\langle \Theta \rangle_{|E_i\rangle} \propto \frac{1}{E_i - E_g}$.*

Proof. Since the minimal eigenvalue of \tilde{H} is 0 with eigenvector $\frac{\sqrt{\Theta^{-1}|g\rangle}}{\langle g|\Theta^{-1}|g\rangle}$, using the lemma above we get that the optimal gap occurs when $\tilde{H} \propto I - \frac{\sqrt{\Theta^{-1}|g\rangle}\langle g|\sqrt{\Theta^{-1}}}{\langle g|\Theta^{-1}|g\rangle}$. Multiplying both sides by $\sqrt{\Theta}$ we obtain $\Theta(H - E_g)\Theta \propto \Theta - \frac{|g\rangle\langle g|}{\langle g|\Theta^{-1}|g\rangle}$. Multiplying then by $H - E_g$ we get $(H - E_g)\Theta(H - E_g)\Theta \propto (H - E_g)\Theta$, which is equivalent to $E\Theta E \propto E$, thus $(E_i - E_g)^2 \langle E_i | \Theta | E_i \rangle \propto E_i - E_g$. This concludes the proof. \square

CK Averages Approximations

Lemma 3. *Consider $\langle \sigma | \psi \rangle \sim \mathcal{N}(0, K)$ and K being the CK, with $\langle \sigma | \psi \rangle \in \mathbb{R}^{2^N}$; then*

$$\mathbb{E} \left(\frac{\langle g | \psi \rangle^2}{\langle \psi | \psi \rangle} \right) = \frac{\mathbb{E}(\langle g | \psi \rangle^2)}{\mathbb{E}(\langle \psi | \psi \rangle)} + \mathcal{O}(N \cdot 2^{-N/2}).$$

Proof. Working with the basis $|s\rangle$, the basis of eigenstates of K

$$\mathbb{E} \left(\frac{\langle g | \psi \rangle^2}{\langle \psi | \psi \rangle} \right) = \sum_s \mathbb{E} \left(\frac{\psi_s^2}{\langle \psi | \psi \rangle} \right) \langle g | s \rangle^2,$$

with $\psi_s^2 \equiv \langle s | \psi \rangle^2$. We assume without loss of generality that the eigenstate with maximal eigenvalue is the state $|+\rangle$, and that the eigenvalues are normalized such that $\langle + | K | + \rangle = 1$. Let us denote $\psi_+^2 = \langle + | \psi \rangle^2$. Then, for any $s \neq +$ we have $\text{Cov}(\psi_s^2, \langle \psi | \psi \rangle) \propto \langle s | K | s \rangle^4$, which, according to the discussion in Sec. III, decays at least as fast as $\sim \frac{1}{2^{4N}}$. For the case that $s = +$ we have $\mathbb{E} \left(\frac{\psi_+^2}{\langle \psi | \psi \rangle} \right) = \mathbb{E} \left(\frac{\psi_+^2}{\psi_+^2 + \xi^2} \right)$ with $\xi^2 = \sum_{s \neq +} \psi_s^2$. Evaluating the Gaussian integral in the complex plane we get $\mathbb{E} \left(\frac{\psi_+^2}{\psi_+^2 + \xi^2} \right) = 1 - A \mathbb{E} \left(\xi e^{-\frac{\xi^2}{2}} \text{erf} \left(\frac{\xi}{\sqrt{2}} \right) \right)$, with A being a positive constant. Using Cauchy-Schwarz we get $\left| \mathbb{E} \left(\frac{\psi_+^2}{\psi_+^2 + \xi^2} \right) - 1 \right|^2 \leq B \mathbb{E}(\xi^2) = B \sum_{s \neq +} \langle s | K | s \rangle$, with B being a positive constant. Since the κ th unique eigenvalue of K decays as $\sim 2^{-N\kappa}$, and since the degeneracy of each subspace is $\binom{N}{|s|}$, using the weak bias property Eq. (12) we have $\sum_{s \neq +} \langle s | K | s \rangle \leq 2 \sum_{k=1}^{N/2} \binom{N}{2k} 2^{-Nk} = (1 + 2^{-N/2})^N - 1$, which for large N approaches $N \cdot 2^{-N/2}$. \square

Convergence

Proof. Theorem 1: Looking at the energy time derivative we get

$$\frac{d\langle E \rangle}{dt} = - \frac{\langle \psi | (H - \langle E \rangle) \Theta (H - \langle E \rangle) | \psi \rangle}{\langle \psi | \psi \rangle^2}.$$

Following [35] we have $\Theta > 0$ and so $\frac{d\langle E \rangle}{dt} \leq 0$, with equality occurring only for $|\psi\rangle \propto |E_i\rangle$. Since $\langle E \rangle$ is bounded (due to H being a bounded operator), convergence is guaranteed. To see the stability of the fixed point we consider the solution of the equation near an eigenstate of H , $|\psi\rangle = |E_i\rangle + \epsilon|\phi\rangle$ with $\epsilon \ll 1$, $\langle g|\phi_0\rangle = 0$, and $\langle \phi_0|\phi_0\rangle = 1$, where $|\phi_0\rangle$ is the initial perturbation. Substituting into Eq. (9) we get $\frac{d|\phi\rangle}{dt} = -\Theta(H - E_i)|\phi\rangle + \mathcal{O}(\epsilon)$. Solving the equation to first order in ϵ we find that

$$|\psi\rangle = |E_i\rangle + \epsilon\sqrt{\Theta}e^{-\sqrt{\Theta}(H-E_i)\sqrt{\Theta}t}\sqrt{\Theta^{-1}}|\phi_0\rangle + \mathcal{O}(\epsilon^2),$$

where we assumed that the norm of the initial state near the fixed point is 1 to first order in ϵ without loss of generality. From the form of the solution the condition for the stability of the fixed point is that the operator $\sqrt{\Theta}(H - E_i)\sqrt{\Theta}$ will be positive semidefinite. One can see that the expectation of the operator over the state $\sqrt{\Theta^{-1}}|g\rangle$ is $\frac{E_g - E_i}{\langle g|\Theta^{-1}|g\rangle}$, which is negative except for the case that the fixed point is proportional to the ground state.

Theorem 2: To simplify the algebra, we assume here, without loss of generality, that $E_g = 0$.

Case (1): For $\langle E \rangle \geq \frac{\Delta}{C}$ we have

$$\frac{d\langle E \rangle}{dt} = -\frac{\langle \psi | ((\langle E \rangle - H) \Theta ((\langle E \rangle - H) | \psi))}{\langle \psi | \psi \rangle^2},$$

multiplying and dividing by $\langle g|\Theta^{-1}|g\rangle$ and using the Cauchy-Schwarz inequality we get

$$\frac{d\langle E \rangle}{dt} \leq -\frac{\langle \psi | g \rangle^2 \langle E \rangle^2}{\langle \psi | \psi \rangle^2 \langle g | \Theta^{-1} | g \rangle},$$

defining $|\tilde{\psi}\rangle$ as the normalized state, $\frac{d\langle E \rangle}{dt} \leq -\frac{\langle \tilde{\psi} | g \rangle^2 \langle E \rangle \Delta}{\langle \psi | \psi \rangle \langle g | \Theta^{-1} | g \rangle C}$.

Using Eq. (9) we have $\frac{d\langle \psi | \Theta^{-1} | \psi \rangle}{dt} = 0$, hence $\langle \psi | \psi \rangle = \frac{\langle \psi_0 | \Theta^{-1} | \psi_0 \rangle}{\langle \psi | \Theta^{-1} | \psi \rangle} \leq \|\Theta\| \langle \psi_0 | \Theta^{-1} | \psi_0 \rangle$, with $|\psi_0\rangle$ the initial state. Assuming without loss of generality that $\langle \psi_0 | \Theta^{-1} | \psi_0 \rangle = 1$ we obtain

$$\frac{d\langle E \rangle}{dt} \leq -\frac{\min(\langle \tilde{\psi} | g \rangle^2) \Delta \langle E \rangle}{C \|\Theta\| \langle g | \Theta^{-1} | g \rangle},$$

which concludes the proof of the first bound.

For the case $\langle E \rangle \leq \frac{\Delta}{C}$ we have

$$\frac{d\langle E \rangle}{dt} \leq -\frac{\langle \psi | g \rangle^2 \langle E \rangle^2}{2 \langle \psi | \psi \rangle^2 \langle g | \Theta^{-1} | g \rangle} - \frac{1}{2d-2} \sum_{i>0}^d \frac{\langle \psi | ((\langle E \rangle - H) \Theta ((\langle E \rangle - H) | \psi)) \langle E_i | \Theta^{-1} | E_i \rangle}{\langle \psi | \psi \rangle^2 \langle E_i | \Theta^{-1} | E_i \rangle},$$

where $d \equiv 2^N$ and $|E_i\rangle$ are the eigenstate of H . Using Cauchy-Schwarz we have

$$\frac{d\langle E \rangle}{dt} \leq -\frac{\langle \psi | g \rangle^2 \langle E \rangle^2}{2 \langle \psi | \psi \rangle^2 \langle g | \Theta^{-1} | g \rangle} - \frac{1}{2d-2} \sum_{i>0} \frac{\langle \psi | E_i \rangle^2 ((\langle E \rangle - E_i))^2}{\langle \psi | \psi \rangle^2 \langle E_i | \Theta^{-1} | E_i \rangle}.$$

Focusing on the sum on the RHS, we have $\sum_{i>0} \frac{\langle \psi | E_i \rangle^2 ((\langle E \rangle - E_i))^2}{\langle \psi | \psi \rangle^2 \langle E_i | \Theta^{-1} | E_i \rangle} \geq \frac{1}{\|\Theta\|} \min_{i \geq 1} \left(\frac{|E_i - \Delta/C|}{\langle i | \Theta^{-1} | i \rangle} \right) \sum_{i>0} \tilde{\psi}_i (E_i - \langle E \rangle) = \frac{1}{\|\Theta\|} \min_{i \geq 1} \left(\frac{|E_i - \Delta/C|}{\langle i | \Theta^{-1} | i \rangle} \right) \tilde{\psi}_g^2 \langle E \rangle$. Thus, overall we get $\frac{d\langle E \rangle}{dt} \leq -\frac{a}{2} \langle E \rangle^2 - b \langle E \rangle$ with a, b defined in Theorem 2. Solving the inequality we arrive at the final result.

Case (2): Using Eq. (9),

$$\frac{d\psi_g}{dt} = \frac{\langle g | \Theta | g \rangle}{\langle \psi | \Theta | \psi \rangle} \langle E \rangle \psi_g \geq \frac{\langle g | \Theta | g \rangle \Delta}{\|\Theta\| C} \psi_g,$$

due to $|g\rangle$ being an eigenstate of Θ . We thus find

$$\psi_g \geq \psi_g(t=0) \exp \left[\frac{\langle g | \Theta | g \rangle \Delta}{\|\Theta\| C} t \right],$$

which implies that

$$\tilde{\psi}_g^2 \geq \frac{\Theta_{\min}}{\|\Theta\|} \tilde{\psi}_g(t=0) \exp \left[\frac{\langle g | \Theta | g \rangle \Delta}{\|\Theta\| C} t \right],$$

since $\min(\langle\psi|\psi\rangle) \geq \Theta_{\min}$. One can then see that $\langle E \rangle = \sum_i \tilde{\psi}_i^2 E_i \leq \sum_{i>0} \psi_i^2 \|H\| = (1 - \tilde{\psi}_g^2) \|H\|$ and employ the fact that $1 - x < \frac{1}{x}$ for every $x > 0$ to get the final bound.

Case (3): Let us start from $\frac{d\langle E \rangle}{dt} = -\frac{\langle\psi|(\langle E \rangle - H)\Theta(\langle E \rangle - H)|\psi\rangle}{\langle\psi|\psi\rangle^2}$. Since $[\Theta, H] = 0$ we have $\frac{d\langle E \rangle}{dt} = -\frac{1}{\langle\psi|\psi\rangle} \sum_i \psi_i^2 (\langle E \rangle - E_i)^2 \Theta_i \leq -\frac{\langle\psi|g\rangle^2 \langle E \rangle^2 \Theta_g}{2\langle\psi|\psi\rangle^2} - \sum_{i>0} \frac{\langle\psi|E_i\rangle^2 (\langle E \rangle - E_i)^2 \Theta_i}{\langle\psi|\psi\rangle^2}$. Continuing the argument as in Case (1) we obtain the result.

Proposition 2: Let us examine $\frac{d\psi_g}{dt} = \frac{1}{\langle\psi|\psi\rangle} \langle g|\Theta(\langle E \rangle - H)|\psi\rangle = \frac{1}{\langle\psi|\psi\rangle} \langle g|\Theta(P_g + P_g^\perp)(\langle E \rangle - H)|\psi\rangle$. If $\frac{1}{2} \langle g|\Theta P_g(\langle E \rangle - H)|\psi\rangle \geq \langle g|\Theta P_g^\perp(\langle E \rangle - H)|\psi\rangle$ then $\frac{d\psi_g}{dt} \geq \frac{1}{2\langle\psi|\psi\rangle} \langle g|\Theta|g\rangle \langle E \rangle \psi_g$ and Case (2) argument follows. In order to satisfy the inequality it is enough to satisfy $\frac{1}{4} \langle g|\Theta|g\rangle^2 \tilde{\psi}_g^2 \langle E \rangle^2 \geq \langle g|\Theta P_g^\perp \Theta|g\rangle (\langle E^2 \rangle - \langle E \rangle^2)$, which is the same as $\frac{1}{4} \frac{\langle g|\Theta|g\rangle^2}{\langle g|\Theta^2|g\rangle - \langle g|\Theta|g\rangle^2} \geq \frac{1}{\tilde{\psi}_g^2} \left(\frac{\langle E^2 \rangle}{\langle E \rangle^2} - 1 \right)$. We can now use $\frac{1}{\tilde{\psi}_g^2} \left(\frac{\langle E^2 \rangle}{\langle E \rangle^2} - 1 \right) \leq \frac{1}{\tilde{\psi}_g^2} \frac{C\|H\|}{\Delta}$. Moreover, if $\frac{d\psi_g}{dt} \geq 0$ then $\tilde{\psi}_g^2 \geq \frac{\psi_g^2}{\|\Theta\|}$. It is therefore easy to see that satisfying the inequality for $t = 0$ is then enough for it to hold for all $t \geq 0$.

Theorem 3: In order to converge, the state must be, at some point in time, arbitrarily close to the ground state. We use the approximation $|\psi\rangle = N(|g\rangle + \epsilon|\phi\rangle)$, where $|\phi\rangle$ is orthogonal to the ground state and its norm is less than unity and $\epsilon \ll 1$. N is the norm, $N = \frac{\langle\psi_0|\Theta^{-1}|\psi_0\rangle}{\langle\psi|\Theta^{-1}|\psi\rangle}$. Writing down Eq. (9) in the discrete time form, under those conditions we find to first order in ϵ that

$$|\psi^{t+1}\rangle = \left[\mathbb{I} - \Delta t \frac{\langle g|\Theta^{-1}|g\rangle}{\langle\psi_0|\Theta^{-1}|\psi_0\rangle} \Theta [H - E_g \mathbb{I}] \right] |\psi^t\rangle + \mathcal{O}(\epsilon).$$

After n steps from some time t we have

$$|\psi^{t+n}\rangle = \left[\mathbb{I} - \Delta t \frac{\langle g|\Theta^{-1}|g\rangle}{\langle\psi_0|\Theta^{-1}|\psi_0\rangle} \Theta [H - E_g \mathbb{I}] \right]^n |\psi^t\rangle + \mathcal{O}(\epsilon),$$

and so one has that all the eigenvalues of the operator $\mathbb{I} - \Delta t \frac{\langle g|\Theta^{-1}|g\rangle}{\langle\psi_0|\Theta^{-1}|\psi_0\rangle} \Theta [H - E_g \mathbb{I}]$ must be smaller than unity in absolute value. A necessary condition for that to hold for all the eigenvalues can be seen to be $\Delta t \leq \frac{\langle\psi_0|\Theta^{-1}|\psi_0\rangle}{\langle g|\Theta^{-1}|g\rangle} \frac{2}{\|\sqrt{\Theta(H - E_g)\sqrt{\Theta}}\|}$. \square

App. C Proofs for Sec. V

Proof. Theorem 4: Assume that $|\psi\rangle$ is a solution of Eq. (9) with a Hamiltonian H and initial condition $|\psi_0\rangle$, so $\frac{d|\psi\rangle}{dt} = \frac{1}{\langle\psi|\psi\rangle} \Theta [(\langle E \rangle - H)|\psi\rangle$. Multiplying both sides by U and defining $|\phi\rangle \equiv U|\psi\rangle$, and $\tilde{H} \equiv UH U^\dagger$, we have $\frac{d|\phi\rangle}{dt} = \frac{1}{\langle\phi|\phi\rangle} U\Theta U^\dagger U [\langle \tilde{E} \rangle - H] U^\dagger U |\psi\rangle$, where we also used $U^\dagger U = I$, so $\langle\phi|\phi\rangle = \langle\psi|\psi\rangle$ and $\langle E \rangle = \frac{\langle\psi|H|\psi\rangle}{\langle\psi|\psi\rangle} = \frac{\langle\phi|H|\phi\rangle}{\langle\phi|\phi\rangle}$. Since $[\Theta, U] = 0$ we get $\frac{d|\phi\rangle}{dt} = \frac{1}{\langle\phi|\phi\rangle} \Theta [\langle \tilde{E} \rangle - \tilde{H}] |\phi\rangle$.

The average initial energy is $\mathbb{E}(\langle E_0 \rangle) = \int \frac{\langle\psi_0|H|\psi_0\rangle}{\langle\psi_0|\psi_0\rangle} \exp[-\frac{1}{2} \langle\psi_0|K^{-1}|\psi_0\rangle] d|\psi_0\rangle$ and the initial average overlap is $\mathbb{E}(\tilde{\psi}_g^2(t=0)) = \int \frac{\langle g|\psi_0\rangle^2}{\langle\psi_0|\psi_0\rangle} \exp[-\frac{1}{2} \langle\psi_0|K^{-1}|\psi_0\rangle] d|\psi_0\rangle$. Changing the integration variable from $|\psi\rangle$ to $|\phi\rangle$ and using the fact that the Jacobian of the transformation is 1, we obtain the result.

Corollary 1: Since the general form of the NTK and CK is $\Theta = \sum_S \alpha_S X_S$ with $S \subset \{1, \dots, N\}$ and α_S being real, then $[\Theta, e^{i\chi}] = 0$ for every $\chi = \sum_S \beta_S X_S$.

Corollary 2: As explained in the main text, altering the signs of β_S and γ_S without altering α_S and the magnitudes of β_S, γ_S can only be done using a unitary of the form X_S , which will always commutes with the NTK and CK.

Proposition 3:

(1) Due to the general form of Θ and K , $\text{Tr}(\Theta\mathcal{H}) = \sum \text{Tr}(\Theta X_S) \alpha_S$, where we used the orthogonality properties of the Pauli matrices. Since Θ and K are assumed to be entry-wise positive, $\text{Tr}(\Theta X_S) \geq 0$, and so if one can only change the signs of α_s , the minimum will be obtained whenever $\text{sgn}(\alpha_s) = -1$, provided that it is attainable.

(2) More formally, the statement can be formulated as: If there is a unitary transformation $V \in \{Z_S\}$ that makes $\alpha_s \leq 0$, then $V = \text{argmax}_{U \in \{Z_S\}} \{\langle g|U^\dagger \Theta U|g\rangle\}$. Writing the ground state of the Hamiltonian in the computational

basis $|g\rangle = \sum_{\sigma} g_{\sigma} |\sigma\rangle$, sign transformations of the form Z_S will only change the signs of g_{σ} but not the absolute values $|g_{\sigma}|$. $\langle g|\Theta|g\rangle = \sum_{\sigma,\sigma'} \Theta_{\sigma,\sigma'} g_{\sigma} g_{\sigma'} \leq \sum_{\sigma,\sigma'} \Theta_{\sigma,\sigma'} |g_{\sigma}| |g_{\sigma'}|$, due to $\Theta_{\sigma,\sigma'} \geq 0$, which implies that the upper bound is obtained if and only if $g_{\sigma} \geq 0$. This situations occurs if and only if the Hamiltonian is stoquastic, which, under the assumptions, occurs only if $\alpha_S \leq 0$.

(3) In the extremely biased case, since $\Theta_{\sigma,\sigma'} \geq 0$, we have $\Theta \approx |+\rangle\langle +| + \mathcal{O}(\epsilon)$ with $\epsilon \ll 1$. Then the learning rate bound can be approximately written as $\frac{\epsilon}{1-(1-\epsilon)\langle g|+\rangle^2} \frac{1}{\langle +|H|+\rangle - E_g}$. The first term is a function of $\sum_{\sigma} g_{\sigma}$, hence it is maximized by the case $g_s \geq 0 \forall s$ (or $g_s \leq 0 \forall s$), which only occurs if $\alpha_s \leq 0$. As for the second term, one can see that $\langle +|H|+\rangle = \text{Tr}(H|+\rangle\langle +|) = \sum_s \text{Tr}(HX_s) = \sum \alpha_s$, which is minimized by $\alpha_s \leq 0$. Thus the whole expression is maximized by having $\alpha_s \leq 0$.

Proposition (4): This statement follows from $\langle g|\Theta|g\rangle = \sum_{\sigma,\sigma'} g_{\sigma} g_{\sigma'} \Theta_{\sigma,\sigma'} \leq \sum_{\sigma,\sigma'} |g_{\sigma}| |g_{\sigma'}| \Theta_{\sigma,\sigma'}$. Without changing the norms the bound is obtained if and only if g_{σ} have the same signs for all σ .

Proposition (5): As written in the main text, $\text{Tr}(H_2\Theta) = \sum_{i,j} J_{i,j}^{(X,X)} \alpha_2 + h_i^{(X)} \alpha_1$, with $\alpha_1, \alpha_2 \geq 0$, since Θ is entry-wise positive. Hence, $\text{Tr}(H_2\Theta) \geq -\sum_{i,j} |J_{i,j}^{(X,X)}| \alpha_2 + |h_i^{(X)}| \alpha_1$. \square

App. D Details of the numerical calculations

Throughout the paper we used the common NTK initialization strategy as defined in [33] with a zero bias initialization.

For each plot with one layer we used $5 \cdot 10^4$ hidden units, and for ones with more or varying number of layers we used $2 \cdot 10^3$, which is still much larger than the number of degrees of freedom. For benchmarks of the convergence times we used systems with $N = 5$, which although small, already allows us to see the predicted trends. For every figure addressing the average initialization we used $N = 9$, except for the case where we vary the number of qubits, where we went to $N = 11$.

The convergence times were measured by the time it takes for the energy or ground state overlap to reach a certain threshold ϵ . For the ground state this time is defined as the smallest time for which $\tilde{\psi}_g \geq 0.95$, while for the energy it is the smallest time for which $\langle E \rangle - E_g \leq \frac{\Delta}{C}$, with Δ being the energy gap and $C = 4$.

Both the NTK and CK were calculated by averaging over initializations. In order to determine the number of samples and hidden units we calculated the relative error of the eigenvalues of each kernel, which is the standard deviation over the mean. We chose a number of samples and hidden units such that the error is less than 1% for all of the eigenvalues.

References

- [1] J. Kempe, A. Kitaev, and O. Regev, “*The complexity of the local hamiltonian problem*,” SIAM Journal on Computing **35**, 1070 (2006).
- [2] M. B. Hastings, “*Solving gapped hamiltonians locally*,” Physical Review B **73**, 085115 (2006).
- [3] J. I. Cirac, D. Pérez-García, N. Schuch, and F. Verstraete, “*Matrix product states and projected entangled pair states: Concepts, symmetries, theorems*,” Reviews of Modern Physics **93**, 045003 (2021).
- [4] G. Carleo and M. Troyer, “*Solving the quantum many-body problem with artificial neural networks*,” Science **355**, 602 (2017).
- [5] X. Gao and L.-M. Duan, “*Efficient representation of quantum many-body states with deep neural networks*,” Nature Communications **8**, 662 (2017).
- [6] G. Torlai, G. Mazzola, J. Carrasquilla, M. Troyer, R. Melko, and G. Carleo, “*Neural-network quantum state tomography*,” Nature Physics **14**, 447 (2018).
- [7] T. S. Cubitt, A. Montanaro, and S. Piddock, “*Universal quantum hamiltonians*,” Proceedings of the National Academy of Sciences **115**, 9497 (2018).
- [8] D. Luo and J. Halverson, “*Infinite neural network quantum states: entanglement and training dynamics*,” Machine Learning: Science and Technology **4**, 025038 (2023).
- [9] X. Liang, W.-Y. Liu, P.-Z. Lin, G.-C. Guo, Y.-S. Zhang, and L. He, “*Solving frustrated quantum many-particle models with convolutional neural networks*,” Physical Review B **98**, 104426 (2018).

- [10] M. Hibat-Allah, M. Ganahl, L. E. Hayward, R. G. Melko, and J. Carrasquilla, “*Recurrent neural network wave functions*,” *Physical Review Research* **2**, 023358 (2020).
- [11] O. Sharir, Y. Levine, N. Wies, G. Carleo, and A. Shashua, “*Deep autoregressive models for the efficient variational simulation of many-body quantum systems*,” *Physical Review Letters* **124**, 020503 (2020).
- [12] T. Westerhout, N. Astrakhantsev, K. S. Tikhonov, M. I. Katsnelson, and A. A. Bagrov, “*Generalization properties of neural network approximations to frustrated magnet ground states*,” *Nature Communications* **11**, 1593 (2020).
- [13] A. Szabó, “*Neural network wave functions and the sign problem*,” *Physical Review Research* **2**, 033075 (2020).
- [14] C.-Y. Park and M. J. Kastoryano, “*Expressive power of complex-valued restricted boltzmann machines for solving nonstoquastic hamiltonians*,” *Physical Review B* **106**, 134437 (2022).
- [15] M. Bukov, M. Schmitt, and M. Dupont, “*Learning the ground state of a non-stoquastic quantum hamiltonian in a rugged neural network landscape*,” *SciPost Physics* **10**, 147 (2021).
- [16] Y. Nomura, “*Helping restricted boltzmann machines with quantum-state representation by restoring symmetry*,” *Journal of Physics: Condensed Matter* **33**, 174003 (2021).
- [17] A. Jacot, F. Gabriel, and C. Hongler, in *Proceedings of the 32nd International Conference on Neural Information Processing Systems*, NIPS’18 (Curran Associates Inc., 2018) pp. 8580–8589.
- [18] J. Lee, Y. Bahri, R. Novak, S. S. Schoenholz, J. Pennington, and J. Sohl-Dickstein, in *International Conference on Learning Representations* (2018).
- [19] R. Novak, L. Xiao, J. Lee, Y. Bahri, G. Yang, J. Hron, D. A. Abolafia, J. Pennington, and J. Sohl-Dickstein, in *International Conference on Learning Representations* (2019).
- [20] R. M. Neal, *Bayesian learning for neural networks* (Springer Science & Business Media, 2012).
- [21] J. Liu, K. Najafi, K. Sharma, F. Tacchino, L. Jiang, and A. Mezzacapo, “*Analytic theory for the dynamics of wide quantum neural networks*,” *Physical Review Letters* **130**, 150601 (2023).
- [22] F. Girardi and G. De Palma, “*Trained quantum neural networks are gaussian processes*,” arXiv preprint arXiv:402.08726 (2024).
- [23] C.-Y. Park and M. J. Kastoryano, “*Geometry of learning neural quantum states*,” *Physical Review Research* **2**, 023232 (2020).
- [24] Z. C. Lipton, J. Berkowitz, and C. Elkan, “*A critical review of recurrent neural networks for sequence learning*,” arXiv preprint arXiv:1506.00019 (2015).
- [25] L. Alzubaidi, J. Zhang, A. J. Humaidi, A. Al-Dujaili, Y. Duan, O. Al-Shamma, J. Santamaría, M. A. Fadhel, M. Al-Amidie, and L. Farhan, “*Review of deep learning: concepts, cnn architectures, challenges, applications, future directions*,” *Journal of Big Data* **8**, 53 (2021).
- [26] K. Hornik, “*Approximation capabilities of multilayer feedforward networks*,” *Neural Networks* **4**, 251 (1991).
- [27] T. Albash and D. A. Lidar, “*Adiabatic quantum computation*,” *Reviews of Modern Physics* **90**, 015002 (2018).
- [28] D. E. Logan, “*Many-body quantum theory in condensed matter physics—an introduction*,” *Journal of Physics A: Mathematical and General* **38**, 1829 (2005).
- [29] J. Klassen and B. M. Terhal, “*Two-local qubit hamiltonians: when are they stoquastic?*” *Quantum* **3**, 139 (2019).
- [30] B. M. Austin, D. Y. Zubarev, and W. A. Lester, “*Quantum monte carlo and related approaches*,” *Chemical Reviews* **112**, 263 (2011).
- [31] J. Klassen, M. Marvian, S. Piddock, M. Ioannou, I. Hen, and B. Terhal, “*Hardness and ease of curing the sign problem for two-local qubit hamiltonians*,” *SIAM Journal on Computing* **49**, 1332 (2020).
- [32] M. Marvian, D. A. Lidar, and I. Hen, “*On the computational complexity of curing non-stoquastic hamiltonians*,” *Nature Communications* **10**, 1571 (2019).

- [33] G. Yang and H. Salman, “A fine-grained spectral perspective on neural networks,” arXiv preprint arXiv:1907.10599 (2019).
- [34] Y. Zhang, Z.-Q. J. Xu, T. Luo, and Z. Ma, “Explicitizing an implicit bias of the frequency principle in two-layer neural networks,” arXiv preprint arXiv:1905.10264 (2019).
- [35] Y. Belfer, A. Geifman, M. Galun, and R. Basri, “Spectral analysis of the neural tangent kernel for deep residual networks,” arXiv preprint arXiv:2104.03093 (2021).
- [36] F. Becca and S. Sorella, *Quantum Monte Carlo Approaches for Correlated Systems* (Cambridge University Press, 2017).
- [37] S. Sorella, “Green function monte carlo with stochastic reconfiguration,” *Physical Review Letters* **80**, 4558 (1998).
- [38] G. Yang, “Scaling limits of wide neural networks with weight sharing: Gaussian process behavior, gradient independence, and neural tangent kernel derivation,” arXiv preprint arXiv:1902.04760 (2019).
- [39] S. Alemohammad, Z. Wang, R. Balestriero, and R. Baraniuk, in *International Conference on Learning Representations* (2021).
- [40] J. Hron, Y. Bahri, J. Sohl-Dickstein, and R. Novak, in *Proceedings of the 37th International Conference on Machine Learning*, ICML’20, Vol. 407 (JMLR.org, 2020) p. 11.
- [41] G. Yang, “Tensor programs ii: Neural tangent kernel for any architecture,” arXiv preprint arXiv:2006.14548 (2020).
- [42] L. Chizat, E. Oyallon, and F. Bach, “On lazy training in differentiable programming,” in *Proceedings of the 33rd International Conference on Neural Information Processing Systems* (Curran Associates Inc., Red Hook, NY, USA, 2019).